AST Trust
Advancing Steam Traction

NEWSLETTER No. 17 - OCT 2021

BURE VALLEY RAILWAY No. 6 'BLICKLING HALL', THE LOCOMOTIVE USED FOR THE BIOCOAL TRIALS IN JUNE - SEE PAGE 12....

CONTENTS

CHAIRMAN'S PIECE
John Hind

Perhaps our conference is a sign that society is taking the first steps back to a normal way of life. It was good to see old friends again and exchange stories and network with a group of like-minded people. We used our Zoom account to broadcast live, though it did challenge IT resources as we had two laptops running – one for the presentation, one for Zoom and all sent out by Grant Soden's mobile phone!

Many thanks to Chris Newman, Cedric Lodge and Grant Soden for the behind the scenes but essential efforts to get the 'show on the road', which was done at relatively short notice, once we understood that events like this would be allowed.

Thanks must go out to our speakers who take the time and effort to prepare a talk. One of the things that gives me great satisfaction is that we give chance for 'newbies presenters' to test their skills in a welcoming environment. It was Alex Powell's first presentation, though you would not have known it. A couple of years ago Tom Kay gave his first ever presentation to us and since then Tom has gone on to join Ricardo Rail, where he will have given several more.

Chris Newman writes later in the Newsletter about the conference. At the conference we saw the first parts that are the results of all the work that Jamie, Richard, Alex and Grant have been doing on Revolution. There is still a long way to go and we have spent just over £4000 of the initial donation of £10000 which we allocated to the manufacture of the rolling chassis.

We have not started formally fundraising for Revolution, pending completion of the design and an artist's impression, but two people have already made funding contributions to the engine. Once we have these then we can start a more aggressive fund-raising campaign, but in the meantime if you would like to donate, please let us know via info@advanced-steam.org

Later in the newsletter our treasurer Paul Hibberd writes about the tax advantages of making charitable donations or leaving a legacy. In a case like Revolution, I personally think it's better to make charitable donation now – there is more chance of seeing it now than in the afterlife!!

MEMBERSHIP MATTERS
Chris Newman

New Members

We welcome the following new members who have joined since our No 16 Newsletter was circulated:

- **Peter Lewis** from Warwickshire. Peter founded and moderated the Steam Tube website and Rail Tube on Facebook. He is currently the newsletter editor and webmaster for WATTRAIN (World Alliance of Tourist Trams and Trains), and has edited and published a photographic volume on the Stratford-upon-Avon and Junction Midland Railway. He also presents two programmes on North Cotswold Community Radio (www.nccr.co.uk).
- **Tim Heeks** from Belgrave Heights, Victoria, Australia. Tim is the Drawing Office Manager and Carriage & Wagon Superintendant at the Puffing Billy Railway. Before emigrating to Australia in 2010, he was Project Design Engineer at Morganite Crucible Limited in Worcester, UK. He has also been a fireman, guard and signalman on the Welsh Highland Railway.
- **Douglas Dick** from Surrey (UK). Douglas holds a Master's Degree in Chemical Engineering and spent his career in various branches of BP (mainly in research). He has been a volunteer driver, fireman and tracklayer on the Ffestiniog Railway, and owns his own 5" gauge locomotive. He currently volunteers on the 2ft gauge Hampton & Kempton Waterworks Rly.

Deaths

We are saddened to report the death of **Nigel Thornley** who had been a member of ASTT since 2016 and was a regular attendee at our conferences. His career was in electronics/electrical engineering and he had been Chairman of Medem UK, specialising in gas detection systems. His passion was the Lancashire and Yorkshire Railway and he was actively involved in the L&Y Railway Society.

Membership Numbers

Membership now stands at 90, broken down as follows:

Full Members:	27	UK members:	64
Associate Members:	58	EU:	13
Student Members:	5	USA	6
		Australasia:	6
Total Membership:	90	China:	1

PUBLICATIONS PAGE
Chris Newman

Book Sales

33 books have been sold in the four months since Newsletter No 16 was circulated. These are listed as follows:

Publisher	Author	Title	Sales since N/L 16	Total Sales
ASTT	L.D. Porta	Porta's Papers Vol 1	3	117
	L.D. Porta	Porta's Papers Vol 2	2	111
	L.D. Porta	Porta's Papers Vol 3	19	62
	Ian Gaylor	Lyn Design Calculations	4	95
	David Wardale	5AT FDCs	1	201
	Alan Fozard	5AT Feasibility Study	0	38
Camden	David Wardale	Red Devil and Other Tales ..	0	260
	Phil Girdlestone	Here be Dragons	0	31
	Jos Koopmans	The Fire Burns Better …	1	5
	L.D. Porta	Advanced Steam Design	1	4
Crimson Lake	Adrian Tester	A Defence of the MR/LMS 4F 0-6-0	1	22
	Adrian Tester	Introduction to Large Lap Valves	1	13

Future Publications

Two more publications remain in the pipeline:

- Volume 4 of Porta's Papers covering boiler water treatment, feedwater heating and boiler water circulation remains a work in progress. Martyn Bane is undertaking the editorial work.
- An Anthology of papers and publications about Livio Dante Porta and his works. It is hoped that this will be in print in advance of (or soon after) the commencement of his centennial year (2022).

The Advanced Steam Traction Trust

is pleased to offer

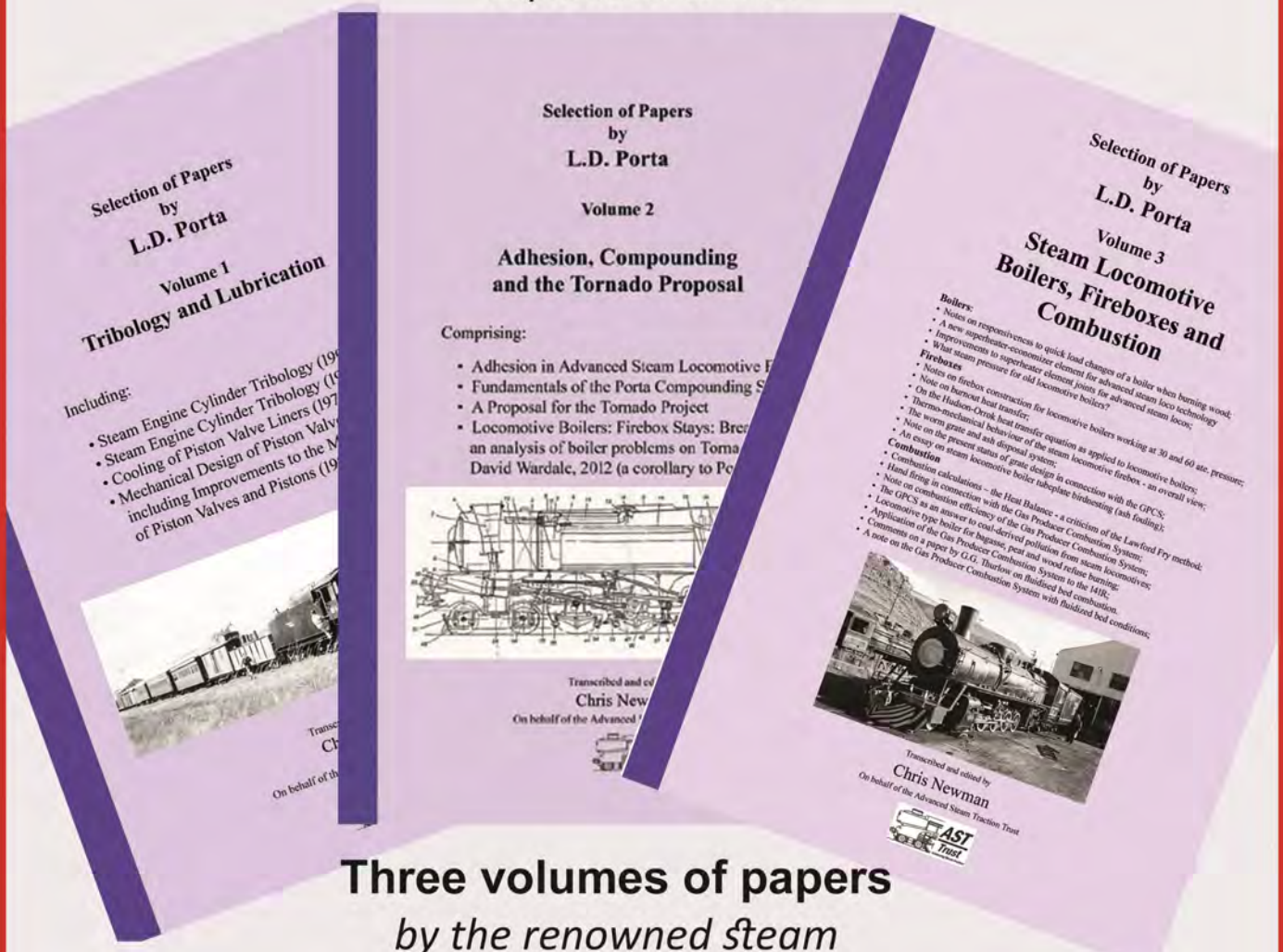

Three volumes of papers

by the renowned steam locomotive engineer

Livio Dante Porta

Members' price £21.60 each

£60 for three volumes (790 pages)

including UK postage

www.advanced-steam.org/books-for-sale

email ***sales@advanced-steam.org***

2021 AUTUMN CONFERENCE
Chris Newman

Our 2021 turned out to be a most successful event in terms of the quality of papers presented. There were concerns that we'd organised too many speakers to fit into the available time but happily our hosts at the Great Central Railway allowed us to carry on until after 6:00pm by when we were ready to leave.

Our seven speakers covered a wide and interesting range of topics as summarised below:

- **David Pawson** gave a presentation on The Zenith of American steam in which he concluded that, despite Porta's contrary opinions, "the Americans built the fastest, most powerful, most rugged designs that outperformed anything else I know of, that could not be significantly bettered in their environment".
- **Andrew Hartland** presented the second part of his investigation into "Why Did BR Give Up On Steam?" in which he looked at the performance levels that steam would have needed to compete with diesels. He concluded that technical solutions should have been available at the time that would have allowed steam to deliver those performance levels had BR been motivation to develop them.
- **Joe Cliffe** presented a paper on "Turbine Locomotives , Condensing and Non-Condensing 1910-1960" in which he outlined the development of turbines during that period, concluding that the only significant problem with Stanier's Turbomotive was that it was a one-off. As a consequence its availability was seriously impaired whenever repairs were needed. Had a fleet of these machines been authorised, the LMS could have invested in the equipment to manufacture the turbines and to have maintain a stock of parts that would have enabled repairs to be implemented quickly.
- **Hendrik Kaptein** presented a paper on "Fireless Steam" in which he argued that the technology could be developed to allow fireless steam locomotives to operate over larger distances than they were normally restricted to. He also pointed out that non-carbon fuels could be used for steam generation, such as iron filings.
- **Alex Powell** presented a paper on "Running on the Main Line with Clan Line" based on his experience as an active member of Clan Line's support crew. He described in detail the preparations that have to be made to ready the locomotive for an outing on the main line, and those for returning and bedding down the locomotive after a day out.
- **John Hind** gave a presentation on "Coal Substitutes" in which he outlined some of the work that ASTT has undertaken on the BVR and elsewhere, testing coal substitute fuels including CPL's ECoal50 (made from 50% anthracite and 50% crushed olive stones).
- **Jamie Keyte** gave an update on the work that he and other ASTT members have been doing in advancing the design and manufacture of components for "*Revolution*". He brought with him three of the locomotive's driving wheels and several frame and suspension components (see photo below). Grant Soden also brought a full-sized "3D print" (in plastic) of a cylinder and valve chest for the locomotive.

It is expected that recordings of all seven presentation will be made available to members via ASTT's website.

17 members were in attendance – a low number compared to 2019 when 50 attended – but it was as many as had been hoped for in these post-Covid times. In fact it was just as well that more didn't turn up

as GCR's small meeting room would not have seated any more. In addition to the 17 present, we also had a number of "virtual" attendees via Zoom.

Present at the conference were the following: Alex Powell, Andrew Hartland, Chris Newman, David Gibson, David Pawson, Geoff Ayers, Graham Shirley, Grant Soden, Hendrik Kaptein, Jamie Keyte, John Hind, Joseph Cliffe, Les Turner, Marcus Harriott, Owen Jordan, Paul Winston, William Powell.

Zoom attendees included: Wolf Fengler from the USA (who joined the meeting at 3:00am his time and stayed through to the end), Tim Heeks from Australia, Richard Mellish and David Nicholson, both from the UK.

Apologies were received from Iain McCall, Cedric Lodge, Chali Chaligha, Chris Parmenter, Ian Gaylor and Roger Waller.

The conference presentations which are now available for viewing on our website. Recording the presentations required some careful juggling by our webmaster, Grant Soden, who managed the Zoom connection. This involved him video-recording the speaker using a remote camera whilst simultaneously changing the PowerPoint slides on Zoom so that our Zoom attendees (who included Wolf Fengler in the US and Tim Heeks in Australia) could see the same images that were being presented to the meeting attendees. It's a great credit to him that he planned and managed such a complicated arrangement with apparent ease. [Note: there is a minor downside to the arrangement in that the top right corner of the screen is taken up with a thumbnail view of the presenter, which obscures a small part of some slides.]

Please note that you will need to log-in with your username and password in order to access the recordings.

2021 Conference Dinner at the Cedars Hotel, Loughborough, 18th Sept.

12 members attended the conference dinner at The Cedars Hotel located beside the GCR's tracks, not far from the station. Alex Powell, Andrew Hartland, Chris Newman, Geoff Ayers, Hendrik Kaptein, Jamie Keyte, John Hind, Les Turner, Marcus Harriott, Paul Winston and William Powell. They were joined by Diana Turner who (with her husband Les) had driven to Loughborough all the way down from Inverness. The excellent meal was enhanced by the sight and sound of GCR's evening trains approaching and departing from Loughborough just outside the dinner tent.

Winding down after the Conference dinner. The GCR's tracks ran right beside the tent.

Conference Outing at the Stapleford Miniature Railway, 19th Sept.

14 members turned up at Stapleford for a day of steam rides. Those present were: Alex Powell, Andrew Taylor, Chris Newman, David Gibson, Geoff Ayers, Grant Soden, Hendrik Kaptein, Jamie Keyte, John Hind, Les Turner, Owen Jordan, Paul Hibberd, Paul Winston and Richard Coleby (who organised the event).

As for the 2020 Stapleford outing, three locomotives were in steam: the Curwen Atlantic; the Nickel Plate "Berkshire" (2-8-4) built by Richard Coleby and celebrating its 50th year at the railway; and the New York Central "Niagara" (4-8-4) built by John Wilks. John's 10¼" gauge P2 No 2001 "Cock o' the North" had had its inaugural run the previous weekend, but was not in steam for our event.

The opportunity was taken to try out two "coal substitute" fuels. CPL's ECoal50 (described above) was tried in the "Berkshire" but did not compare well with Welsh Ffos-y-fran coal. It was felt that if the lump size had been smaller and had the driver more time to practice with it, it would have performed better.

(Left) Richard Coleby's 50-year-old Nickel Plate "Berkshire" - fired up with E Coal 50 fuel (right)

A more successful trial was conducted on the Curwen Atlantic using a fuel based on "biogenic" waste material provided by a Dutch manufacturer which Richard Coleby had mixed with additives and re-formed into highly compressed "pucks". It remains to be seen whether a successful coal substitute can be developed from this material but the trial exposed potential problems with smoke emissions.

Richard's compressed pucks containing biogenic waste material and a binding agent. These burned fiercely and held together as they burned, but they emitted more smoke than desirable.

Richard's fuel "pucks" create a good fire in the Curwen Atlantic, but give off a lot of smoke from the chimney. (Richard Coleby at the regulator.)

Wheels and frame/suspension components for Revolution on display, as manufactured by Jamie Keyte. It is hoped that a rolling chassis may be completed before ASTT's next visit to Stapleford.

In addition to rides on the railway, Jamie Keyte had brought his 1884 *Invicta* traction engine which members took turns at driving on the road outside the SMR's entrance gate.

David Gibson stands beside Jamie's 1884 traction engine while Alex Powell gets to grips with the steering mechanism.

GIFT AID & LEGACIES
Paul Hibberd

Gift Aid

If any of our members are higher rate or additional rate taxpayers, they can get personal benefits from a charitable donation for example:-

a) If higher rate tax payer donates £1,000 to a charity. The charity receives £1,250. But the donor gets £200 back. The donor can keep this or donate the £200 he receives back to the charity in which case the charity will receive a total of £1500.

b) if an additional rate tax payer donates £1,000, they would get £250 back instead of £200. Again the donor can keep this or donate back to the charity in which case it receives £1562.50.

If anyone is earning between £100,000 and £125,140 per year the combined effect of the normal tax relief and avoiding tax free personal allowance reduction gives an effective rate of tax relief of 60% - so if anybody is interested in a charity it's a no brainer to put money into a charity.

Legacies

There is a specific exemption from inheritance tax where funds pass to charities. The exemption from funds passing on death to a charity from an estate that is liable to inheritance tax is 40% so a bequest to a charity of £10,000 would only cost other potential beneficiaries of the will £6,000.

There is another case where, if a member receives a legacy they can choose to pass this onto a charity and can effect the transfer as a deed of variation within two years of the date of death. This would enable the gift to be treated as if it had been made by the deceased person and can therefore benefit from the general charitable tax exemption- thereby it could reduce any inheritance tax on the estate of the deceased.

In addition when somebody dies and 10% or more of the 'net estate' (after inheritance tax exemptions, reliefs and the nil rate band) is left to charity the current rate of inheritance tax is reduced from 40% to 36%. So if the 36% applies to say £500,000 then relatives etc. will pay 4% less in inheritance tax which, in this case, would amount to £20,000 less going to the Treasury.

These are complex areas and Paul can give guidance on specific issues. Contact Paul at paul.hibberd@advanced-steam.org

BIOCOAL UPDATE
John Hind

Bure Valley Trials

In June, Ian Gaylor, John Scott and myself were at the Bure Valley Railway conducting a series of tests spread over two days on 3 fuels provided by Coal Products and compared them with coal from Ffos-y-fran. The basis of the tests was the protocol developed by Ian with inputs from Richard Coleby and myself. The tests measured the fuel and water consumption over a round trip, by the simple means of weighing the buckets of fuel used and measuring on the engine the water level at the start and finish of every round trip – as we know the tank dimensions, the quantity used can be calculated. We also measured the smokebox vacuum as the boiler is a new design by Ian Gaylor, who needed data to confirm boiler combustion rates.

The four fuels tested were Ffos-y-fran coal from South Wales (as a baseline) and from Coal Products Limited; Ecoal50, Brite Flame and Homefire Ovals.

The tests took place on Friday 11/6/21 and Monday 14/6/21, as being low season, the BVR was not running on Fridays or Mondays, but was operating at weekends. On each day there were two return trips, one in the morning and one in the afternoon.

The line is nine miles long switchback with the engine working and then coasting downhill or slowing for level crossings.

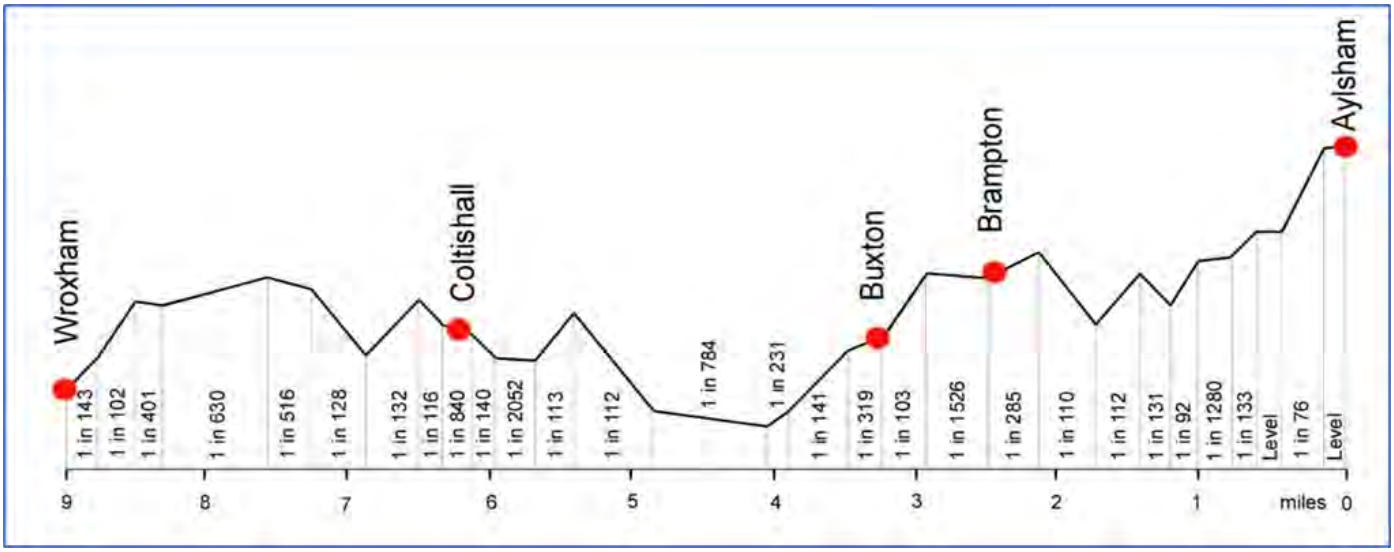

The engine we used was 'Blickling Hall' and for the runs we had the same driver – Scott Bunting. Scott's driving style is remarkably consistent – all the runs were timed and all within a minute of the scheduled time of 45 minutes. Ian Gaylor was the footplate observer and John Scott and I travelled on the train, with myself managing the data logger. As we do on all these trips Mike Horne checked the calibration of the vacuum transducers before and after the tests.

On the Friday we ran with Ffos-y-fran and the Ecoal50. We were joined by Steve Oates – CEO of the Heritage Railway Association and Joanna Dobell who is PA to Sir Peter Hendy, Chairman of Network Rail.

Ian Gaylor and Scott Bunting loading weighed buckets of fuel

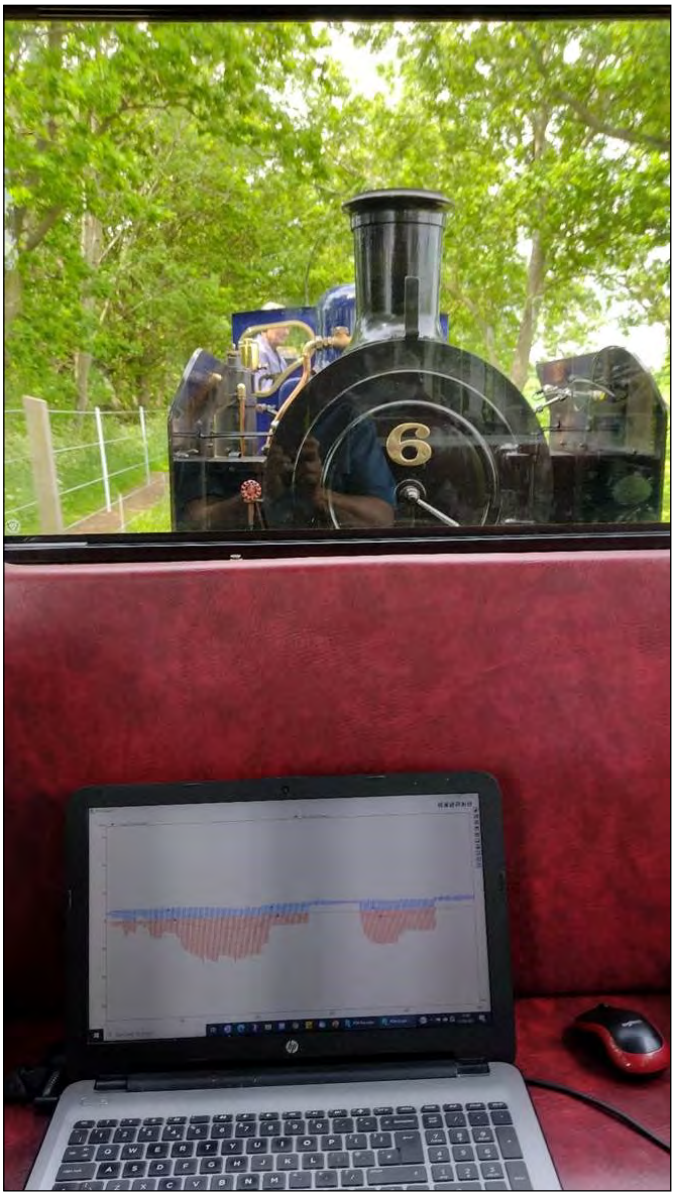

With Vacuum Transducer and Data Logger Connected

Joanna's father, Malcolm Dobell came along as well. Malcolm is an ex-Chairman of the Railway Division of the Institution of Mechanical Engineers, whose career never involved in him steam, so John Scott was able to give him an introduction to these 'interesting' machines.

On the Monday, we tested the Brite flame and the Homefire Ovals.

The Ecoal50 was the second generation of the fuel produced by Coal Products and has moved on from the fuel tested at Stapleford in 2019. It requires a thicker firebed than Ffos-y-fran, which was discovered by Scott on the outward run, which was not going very well until Scott suggested tried trying a thicker fire, which turned the test round.

The downside to Ecoal50 is the cost – in June and prices will have changed since then it was double the price of Russian coal and 50% more than Ffos-y-fran.

It is made up of 50% olive husks which is a waste product from making olive oil and is imported from Spain. The remainder anthracite. Its green credentials are better than coal, but from a railway's point of view you will need more of it to perform the same duties and it will cost you more. In the railway application it is not giving a 50% reduction in CO_2.

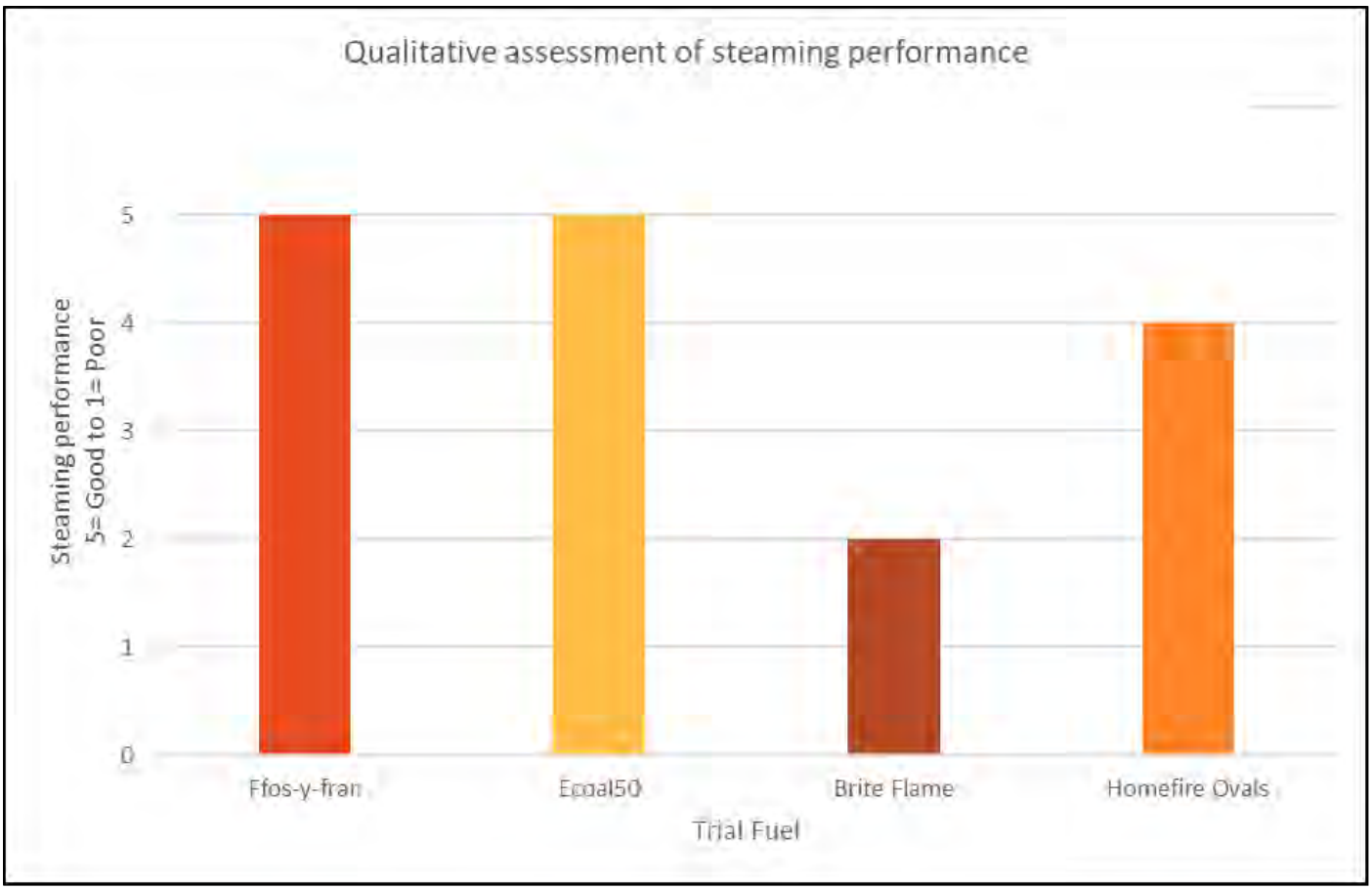
Qualitative assessment of steaming performance
Steaming performance
5= Good to 1= Poor
5
4
3
2
1
0
Ffos-y-fran
Ecoal50
Brite Flame
Homefire Ovals
Trial Fuel

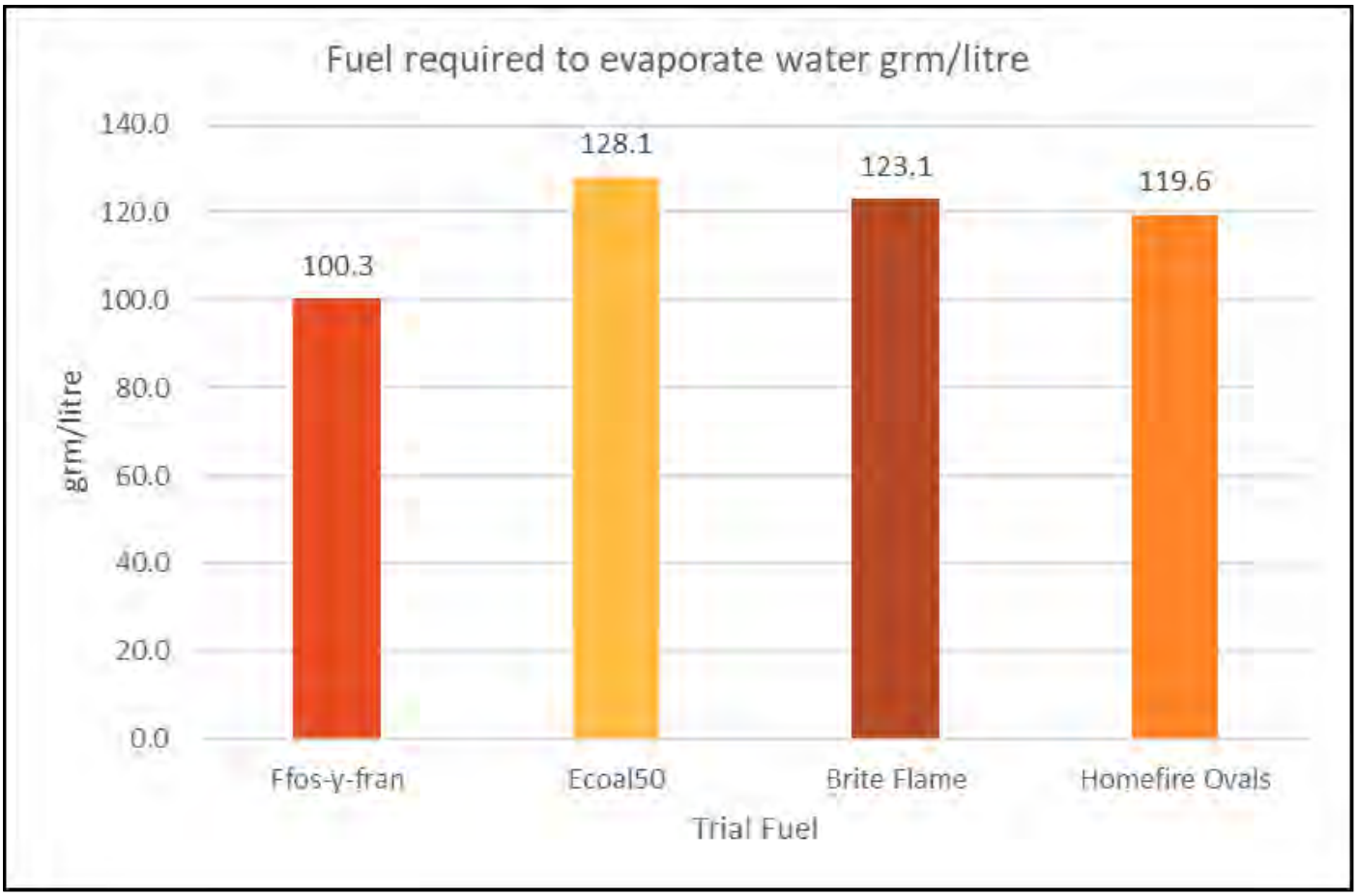
Fuel required to evaporate water grm/litre
grm/litre
140.0
120.0
100.0
80.0
60.0
40.0
20.0
0.0
100.3
128.1
123.1
119.6
Ffos-y-fran
Ecoal50
Brite Flame
Homefire Ovals
Trial Fuel

Ecoal 50 in service

The results from the tests and computer modelling showed that the engine was working burning 53.3 lbs/ sq ft grate/hr, this compares with 80-120 lbs/sqft grate/hr found on demanding work e.g., continuous steeply graded lines often using relatively small locomotives with large loads.

Ourselves and Steve Oates of the HRA have had a meeting with Coal Products this week to feedback results and the plan is to go back to the Bure Valley and run a heavier train to load up Blickling Hall, which is capable of hauling the heavier load. This will increase the burning rate and see whether the fuel performs under more demanding conditions.

As yet we are not convinced Ecoal50 is suitable for standard gauge engines, primarily because of its small size, which is suitable for narrow gauge engines with smaller gaps between the firebars.

In parallel with this Coal Products will be looking at how they can modify their product to suit locomotives – they are already working with blacksmiths to develop a product and are keen to be involved in supplying fuel to the heritage steam sector, which although a diverse sector with lots of small consumers and few big ones, currently consumes 35000 tons a year of coal.

The next set of trials are due to take place on the 23rd/24th of November at the BVR using No6 'Blickling Hall' on one day and No1 'Wroxham Broad' on the second day, so that we can start to see how the fuel performs on other engines.

We have been asked to give an update to the Heritage Railway's Autumn Management Seminar on Tuesday 2/11/21 on the BVR trials, this will be based on the presentation used at our conference.

Other Coal Alternatives

We are still waiting to hear from the USA's Coalition for Sustainable Rail and the University of Minnesota the costs of a small quantity of their bio-coal.

While we were at the Stapleford Miniature Railway on the Sunday of our conference, we took the opportunity to have a bit of 'burn in' with the N+P fuel that was mentioned in the last newsletter. Chris reports on these elsewhere in the newsletter and we will be feeding back results to N+P in the next few weeks.

A RESPONSE TO COMMENT ON SOME COMMENTS

Martin Johnson

I would like to give my full replies to Dr Koopmans' comments as published in ASTT Newsletter 16. These are a slightly modified version of what I sent to Dr. Koopmans in February. Figure numbers and section numbers in the following reply refer to those used in Part 1 of my articles.

2.1. Lengthened chimney

"Why is the idea that a multiple orifice system can be modelled by a single one an “assertion”? "

IF the multiple orifice arrangement is a true representation of a single one, as for example in the case of a double chimney compared to one, then generally the "assertion" is true, aside from minor Reynolds number corrections. However, where multiple orifices are installed in a single chimney the velocity profiles and planes of fluid shear have been significantly changed, so the two cases are no longer "scale models" of each other.

2.3 Multiple orifice single Chimney

"The problem described about the taper reduction was treated during the ASTT lecture with slide 21."

I think this might be an incorrect slide number; from the video it appears to be Slide 16 at around 23 minutes. Nevertheless, I stand by my calculations of Cpi and Cpm for the three cases presented. Based on the video (but struggling with sound quality) Dr. Koopmans seems to agree that Cpm would not change, but does not offer an explanation of why performance would improve over a single nozzle chimney. Variations in Cpi or Cpm do not account for the improvement of a given diffuser by using multiple orifices according to the published calculation method (ASTT lecture Slide 23 - "For a double chimney calculate Cpm from a L/D ratio sqrt(2) larger, 141%" i.e. square root number of orifices, but Area Ratio must remain constant). In Section 4 of my article I gave a coherent explanation of why multiple orifices do give improved performance.

3. Diffusers

I agree that small angles of taper are probably a better mistake to make than too large a taper. I think the GWR 1/14 taper (4 degrees) is rather conservative, but Cox points out that anything above 6 degrees tends to be unstable. My views on the fashion for diffuser angles of 10 deg. and more are set out in the article. I am completely unconvinced by Mr. Day's explanation of why his angled jets work with large taper angles, but I could be convinced of an alternative explanation IF properly controlled tests showed that Mr. Day's geometry did result suppressing flow separation in a wide angle diffuser.

3.1 Diffuser inlet conditions

I cannot agree that inlet conditions in a chimney are OK for a diffuser. Having used similar pitot methods that Young used to determine his velocity profiles (on other work), I must warn that it can be difficult to get good results, particularly near walls. I note that Young devotes some 7 pages (126 to 133) justifying and exploring difficulties with his pitot exploration methods. For comparison, the following figure shows a measured velocity profile at 6 nozzle diameters downstream of the nozzle face of an air on air jet. The experiment used a pitot probe, but in open space and with air as the working fluid, accuracy will be greatly improved. I don't view the curve as an acceptable (near uniform) inlet velocity profile to a diffuser.

Fig. 4 shows that there is a difference in diffuser performance, and I agree that the difference is small; however, the difference in inlet conditions for which the figure is drawn is also small compared to the highly disturbed free jet velocity profile in a chimney.

"(Note that K_d of 0.6 probably has a drawing error compared to figure 1, as also the C_{pm} of 0.45 in the graph of Macdonald.)" I am not sure what your point is here. I would agree that probably the plotting for Fig 1 and Fig 4 (Miller's not mine), (which was done in the days of hand drawn graphs), may be slightly in error in places.

"Since multiple orifices only diminish the peaks and valleys of the exit velocity distribution I regarded the diffuser data usable." My paper shows why the velocity distribution will decay faster with multiple orifices in terms of distance travelled (Section 4.2). However, since the usual approach is to base blast orifice to throat distance on a fixed number of orifice diameters (typically 6 - 7), the peak and trough values at the chimney throat will be identical for both cases. That is the similarity principle at work!

3.2 Diffuser size

I too have built a "Rob Roy" and can confirm it is a terrible steamer as designed. The rest of the design was equally poor. I am sure a 4 nozzle blast, plus a throat and diffuser would improve matters.

My comments on diffuser size were to point out that there are corrections to be made to the published diffuser data to account for absolute size. They are usually presented as a correction factor based on Reynolds number.

As an aside, 1970 model locomotive designs still typically had parallel chimneys and frequently the blast orifice to throat ratio was well away from optimum. Bert Perryman published the Ell "formula" in Model Engineer in the early 1970's which progressed things quite a lot.

3.3. Excess diffusion

I think we agree on this. The article on page 28 of Newsletter 16 by Steve Rapley adds further weight to the argument, although I admit to not having fully digested the detail in the article.

4 Improved front end theory

While momentum exchange is undoubtedly the mechanism at play, it is not necessarily the best calculation tool. If momentum theory is used, a calculation of wall force must be made on a tapered chimney, which depends on an assumed pressure distribution. If kinetic energy is used as a calculation basis, no such problem arises.

It is not feasible to "take care of a uniform exit velocity profile" if we do not account for non uniformity of that velocity profile in calculations. That is effectively saying "we make sure the exit profile is correct by ignoring it". In my first article, I show why the profile improves more rapidly with chimney height in a multi orifice system. I intend to go on and show how the classic kinetic energy based equations (E.g. Porta) can be modified to account for non uniform profiles.

5. The Giesl

"Giesl himself noted in one of his texts that that was because of the longer exhaust channel below the orifice. His orifices are individually adjustable so that each one supplies the same flow." Thank you for that; do you mean the exhaust channel within the nozzle "block" leading to the end orifice? If so, that is confusing, since you would normally get more flow to the end nozzle such a system (As flow is taken from other nozzles, flow in the manifold reduces along with velocity. Since Bernoulli applies, static pressure must increase which causes greater flow in the end orifice).

6. Conclusion

"Since my calculations show so little difference between the calculated and the measured results, I wonder why this is so if they are regarded as “flawed”, misinterpreted and unsound reasoning. .....**Of those tests almost all result in a better performance than the test results show**."

So there is a consistent shift between measured and calculated results - indicating a shortcoming in the theory. I agree that the effect is due to the assumption of uniform velocity fields where they are not uniform. I would also agree that any changes to the theory are likely to have relatively small effects on blast orifice diameter for a given duty, for example.

My aim is to give a better understanding to all interested parties of the fundamental fluid flow principles at work in the system. If we do not grasp that, then we can never move forward with better designs.

SOME COMMENTS ON LOCOMOTIVE FRONT END DESIGN PART 3

Martin Johnson

Errata:

I referred in Section 1.2 of Part 2 to supersonic conditions commencing at 8 psig. That should be 11 psig. I include the calculation of that number in this article.

1. THE ENTHALPY - ENTROPY DIAGRAM

I will be making extensive reference to this type of diagram in this article, so offer the following crash course for those that may not be familiar with them. The presentation is a bit daunting for those not familiar with such charts, so I have produced the simplified guide shown in Figure 1 which shows a simplified enthalpy - entropy diagram. It shows the general form of 4 sets of lines usually shown in addition to the usual grid. They are:

- constant pressure (black) - expressed in Bar absolute.
- constant temperature (blue) - temperature and pressure measurements are usually used together to determine enthalpy and entropy of a given steam condition.
- constant dryness (red dotted) - a wet steam is defined by the percentage of dry steam, the remainder being water at the saturation temperature.
- saturation line (red solid) - the line at which steam is neither superheated nor wet.

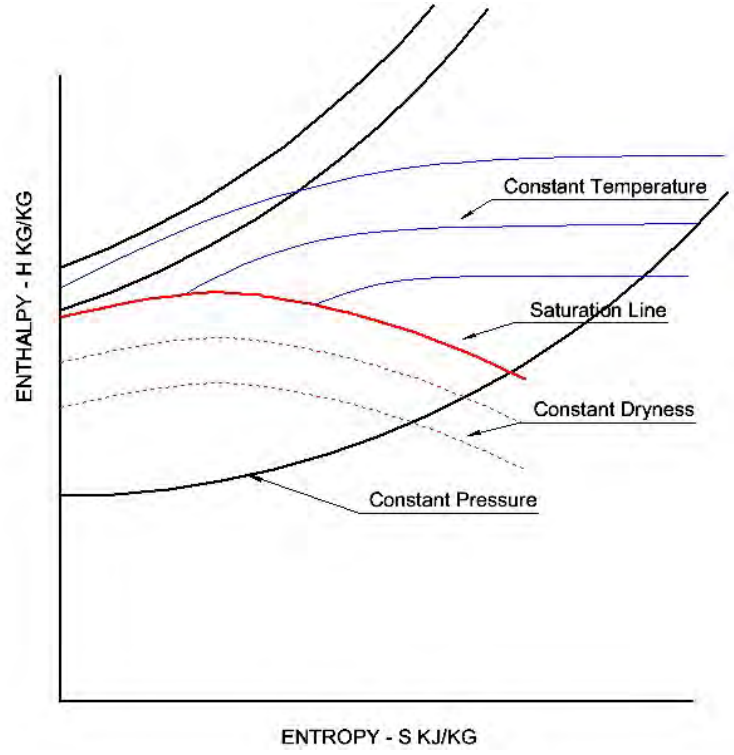

Figure 1: Enthalpy - Entropy chart as usually presented for steam

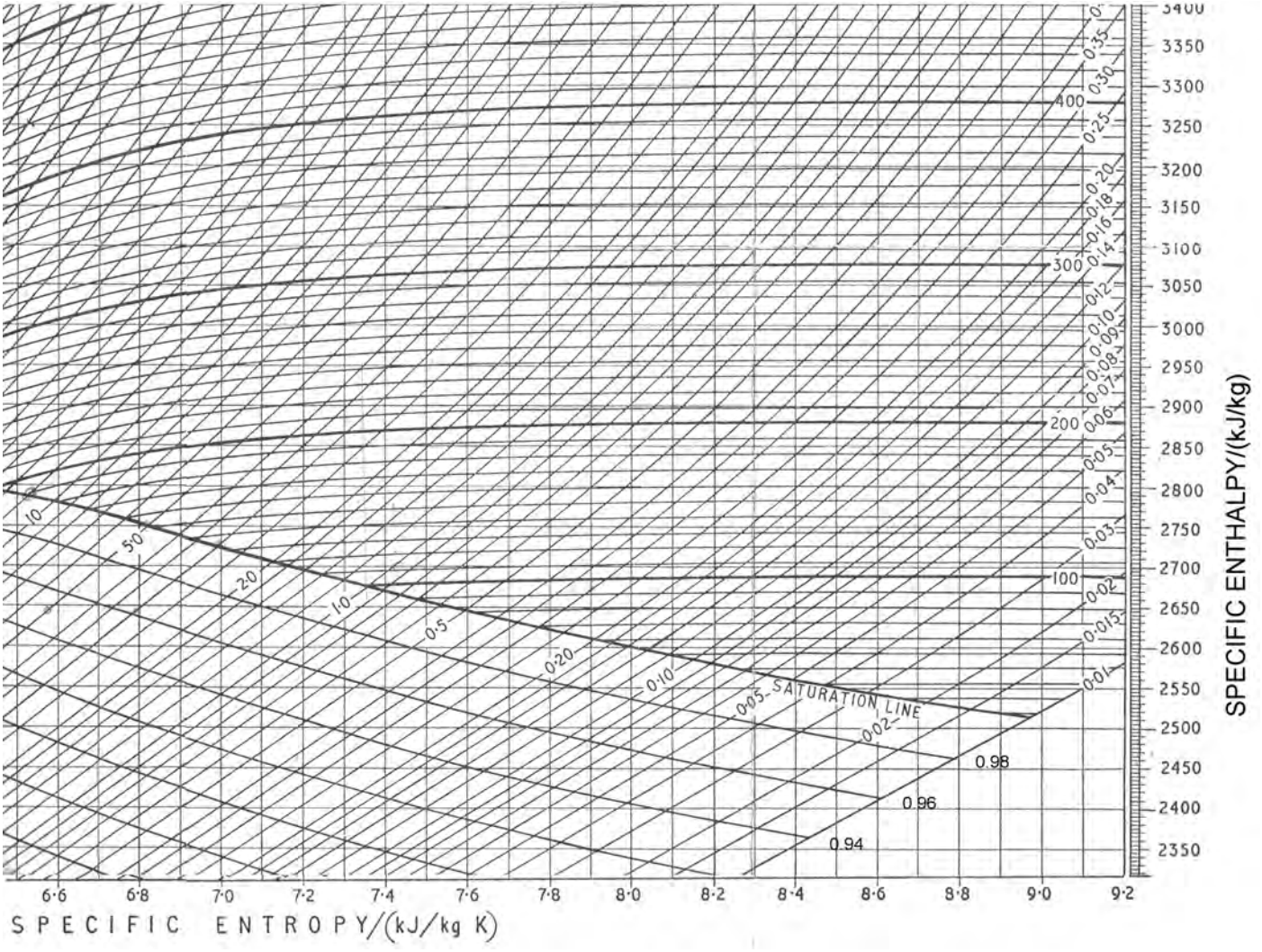

Figure 2: Extract from Enthalpy - Entropy chart, covering the area of interest in locomotive exhaust calculations.

As an example, every schoolboy knows that saturated steam at atmospheric pressure (1 Bar Abs) has a temperature of 100 degrees C. That point lays on the saturation line and the enthalpy at that point is 2675 kJ/kg and the entropy is 7.36 kJ/kg.

2. NOZZLE CALCULATIONS

This section will set out the methods of calculating the performance of a nozzle, including corrections to include real flow effects.

2.1. A Perfect Nozzle

A nozzle converts energy within the steam to kinetic energy according to Bernoulli's theory. Steam is a compressible fluid, but does not approximate very well to a perfect gas. Therefore, internal energy of steam is usually represented by the term "enthalpy" which includes the thermal energy and pressure energy. At the most basic level, if there is zero inlet velocity (i.e. a very large pipe leading to the nozzle) the terminal velocity leaving a nozzle of any sort is:

$$V = \sqrt{2\Delta H}$$

where V = Exit velocity [m/s]

ΔH = Change in enthalpy from inlet to outlet of the nozzle [joules/kg] Note that steam tables usually quote H in KILOjoules/kg.

The total mass flow is given by:

$$M = \rho V A$$

Where:

M = Mass flow per unit time [kg/s]

A = Relevant area of nozzle [m^2]

ρ = Density of steam [kg/m^3]

We now have to consider what is meant by the enthalpy drop from inlet to outlet, and what would be the correct density and area to use. The enthalpy drop is best represented on an enthalpy - entropy diagram for steam.

The diagram in Figure 3 shows a simplified diagram without temperature, saturation or wetness lines, but includes enthalpy drop lines for a nozzle.

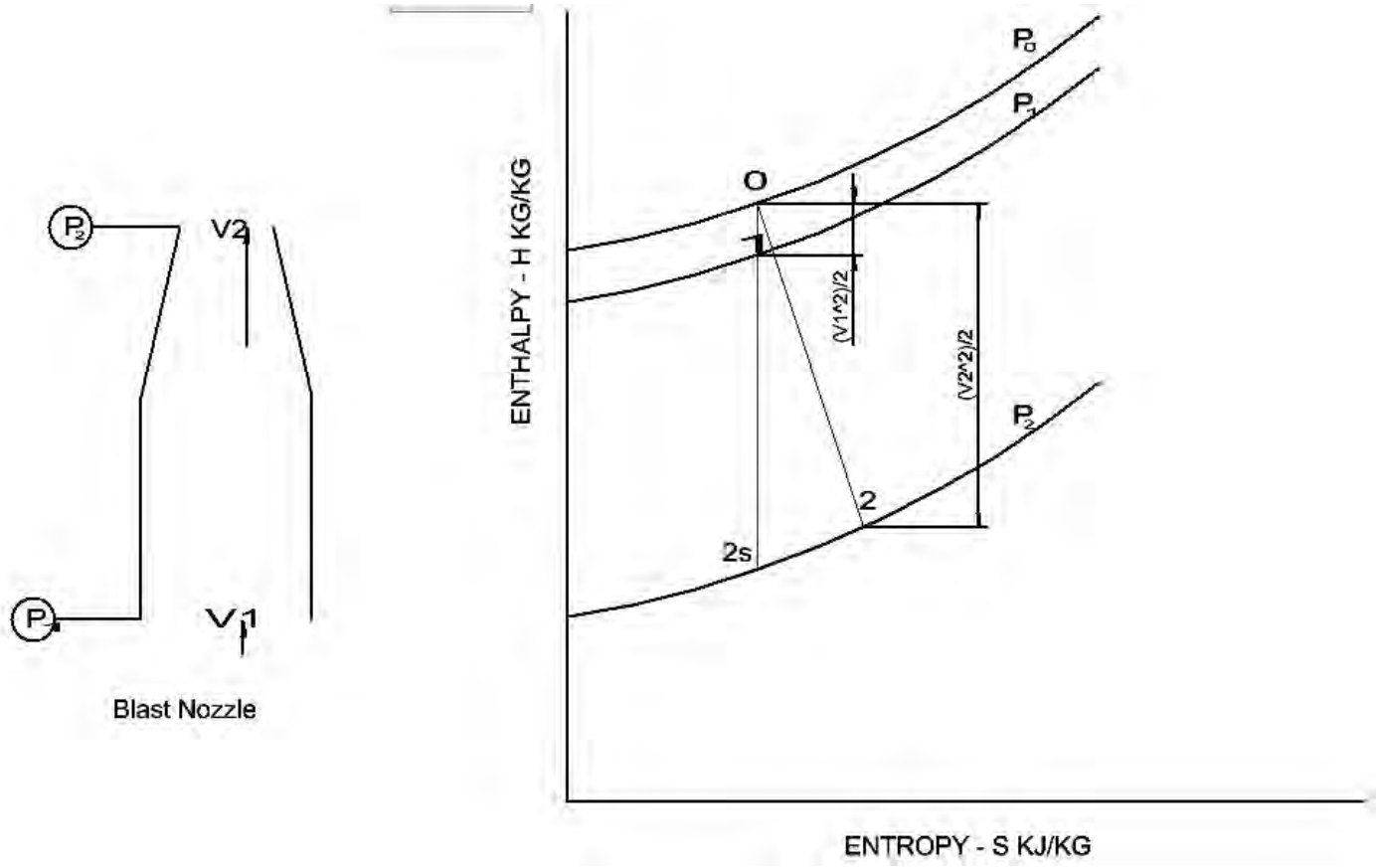

Figure 3: Blast nozzle showing enthalpy - entropy diagram for real nozzle

Figure 3 shows a simple tapered nozzle with an entry velocity, V_1 and exit velocity V_2 plus the associated diagram of enthalpy drop. If we have a perfect nozzle and start from a large vessel at pressure p_0, expanding to a pressure p_2, then the enthalpy drop would be a vertical line from point 0 to 2s.

For the purposes of calculating mass flow, the relevant area would be the exit plane of the nozzle, and the density would be that relevant at pressure P_2 and entropy as shown at 2s.

2.2 The Inlet Velocity Question

The first problem is that there is nowhere in a locomotive exhaust system where the velocity is near zero, so usually when we look at historical test results of exhaust steam pressure, it is equivalent to p_1 NOT p_0. There is seldom any record of what cross section the exhaust was at the point of measurement (See note below *), so the velocity at the plane of measurement is not known, hence pressure p_0 is not precisely known and hence the true enthalpy drop of the exhaust steam is not known.

D. Pawson supplied me evidence of a major argument between E.S. Cox and S.O. Ell in working steam days; the implication was that Ell was obtaining unduly favourable exhaust pressure results by putting the exhaust pressure tapping at a high velocity area. One thing is certain - if you analyse results using p_1 in lieu of p_0, misleading conclusions will result.

As a practical example, Young's tests are well documented (Ref. 4.3) and a careful study of the test set up shows that for a quoted nozzle pressure (p_0) of 8 psi, the p_0 pressure would be 8.5 psi.

Note * - It may be that if one carefully researched original test logs from Rugby, Altoona or wherever, a cross section could be found or it may transpire that a pitot style pressure tapping was used. Few undertake such detailed historical research to determine such details. However, the lesson for present day researchers is very clear - record every detail about the pressure measurement location!

In theory the exhaust enthalpy can be determined from engine inlet enthalpy less work done, or dynamic pressure might be determined from indicator diagrams. I am of the opinion that in both cases experimental error would cloud any conclusions about performance of the front end.

2.3 Nozzle Efficiency

Real nozzles have surface friction and uncontrolled turbulence which leads to energy losses. The friction and turbulence are dissipated as a temperature increase in the fluid, which increases the fluid entropy. So rather than the enthalpy drop being a vertical line from point 0 to 2s, the actual enthalpy drop is between points 0 and 2 on Figure 3. The efficiency with which a nozzle converts enthalpy to velocity energy is defined by C_v (See Section 2.2 of Part 2) which is defined as:

$$C_v = \frac{(h_0 - h_2)}{(h_0 - h_{2s})}$$

Where:

C_v = Velocity coefficient, also known as nozzle efficiency [dimensionless]

h = Enthalpy [kJ/kg]

Subscripts refer to position 0, 2 or 2s on Figure 3.

Typical values for C_v (0.97 to 0.99) for a nozzle (in isolation) were discussed in Section 2.2 of Part 2 and if C_v is known, the velocity leaving a nozzle accounting for friction becomes:

$$V_2 = \sqrt{[C_v 2(h_0 - h_{2s})]}$$

However, if we consider the friction losses across a complete exhaust system which probably includes several right angle bends and two Tee pieces to join both ends of a 2 cylinder locomotive to the blast nozzle, then the overall C_v value would become much lower.

For mass flow calculation, the relevant area of a real nozzle is that at the vena contracta, which is C_c A

(discussed in Section 2.2 of the last article) and the density is at pressure p_2, point 2 in Figure 3:

$$M = \rho_{p2} V_2 C_c A$$

2.4 Supersonic Performance

The equations and methods as set out above only apply when flow is less than the speed of sound. However, once pressure upstream of a nozzle reaches a certain value, the flow in the nozzle will become sonic (also known as "choked").

A Note about sonic calculations for steam

The flow of steam in a nozzle is very complex, and is usually approximated to a perfect gas to simplify the problem. So properties are defined in terms of stagnation pressure and temperature instead of enthalpy. However, whereas the ratio of specific heats is constant for a perfect gas (and nearly constant for a real gas when well above the saturation line) the ratio of specific heats for steam depends on the steam state. Typical values are:

	Ratio of Specific Heats γ
Air (for comparison)	1.4
Superheated steam	1.3
Saturated steam	1.135 - different sources quote different values.
Wet steam	1.035 + 0.1(x) where x is the dryness fraction 1 for saturated steam. Valid for 0.8<x<1

2.4.1 Critical Pressure

I have re-arranged the following widely quoted formula so that it is more relevant to the case where downstream pressure remains near constant (approximately atmospheric), but upstream pressure is varied. The critical upstream pressure is found from:

$$p_0 = \frac{p_c}{\left[\frac{2}{(\gamma+1)}\right]^{\left(\frac{\gamma}{(\gamma-1)}\right)}}$$

where:

P_c = Critical pressure at which flow becomes sonic [Absolute total pressure]

P_0 = Static upstream pressure [Absolute total pressure, same units as above]

γ = Ratio of specific heats

Flow will become choked (i.e. sonic or Mach =1) when p_c equals the downstream pressure, which is approximately 14.7 psi absolute in a smokebox (ignoring the draught requirement). Substituting 1.3 for γ. flow would be Thus flow becomes sonic if p_0 rises above 26.9 psia (superheated steam) or for γ = 1.135,

p_0 would be 24.9 psia for saturated steam. Once this happens, the useful energy released is only that between P_0 and P_c, NOT that between P_0 and P_2. The remaining energy drop between P_c and P_2 is dissipated as turbulence within a sonic shock wave. So my statement in Section 1.2 of Part 2 should have read flow becomes sonic when the upstream pressure reaches approximately 10.2 to 12.2 psi, depending on steam condition.

2.4.2 Beyond the Critical Limit

For a plain nozzle (convergent only) working beyond the critical limit (i.e. at inlet pressures greater than around 11 psig and outlet pressures of atmospheric) the effective pressure drop is progressively reduced

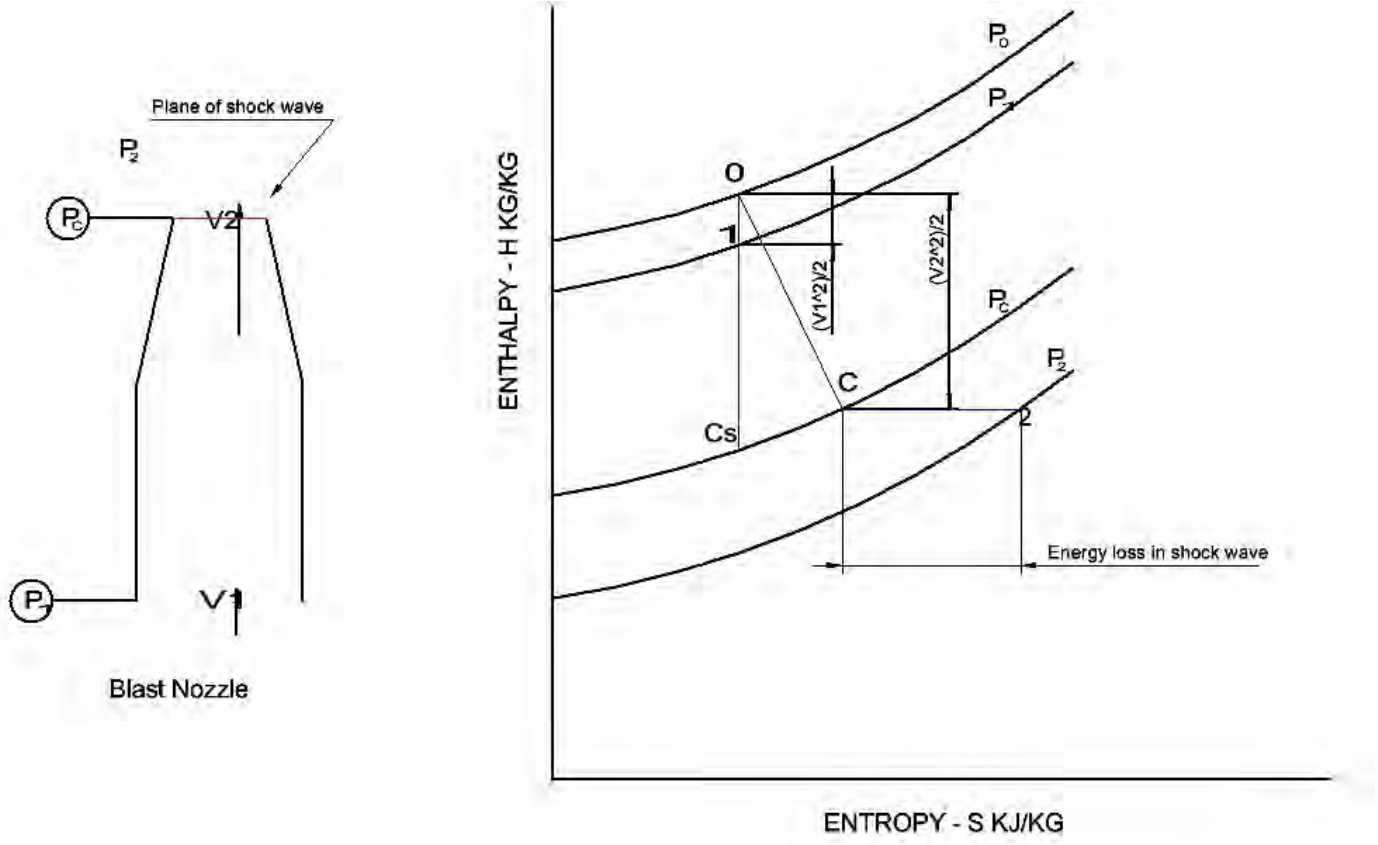

and the enthalpy - entropy diagram is as shown in Figure 4. This shows that the nozzle works as before down to the CRITICAL PRESSURE (Not P_2). The remaining pressure drop to P_2 in the smokebox is by a sonic shock which achieves no useful increase in jet velocity, but converts the energy into low grade heat thus increasing enthalpy.

Figure 4: Enthalpy - Entropy diagram for convergent nozzle working above the critical pressure drop.

So in summary, the velocity is given by:

$$V_2 = \sqrt{[C_v 2(h_0 - h_C)]}$$

and the mass flow is given by:

$$M = \rho_c V_2 C_c A$$

Figure 5 shows how the critical pressure starts to increase above an inlet pressure of 1.8 Bar abs (11.7psi gauge). The energy waste in the shock wave becomes progressively greater, rising to 0.65 Bar wasted

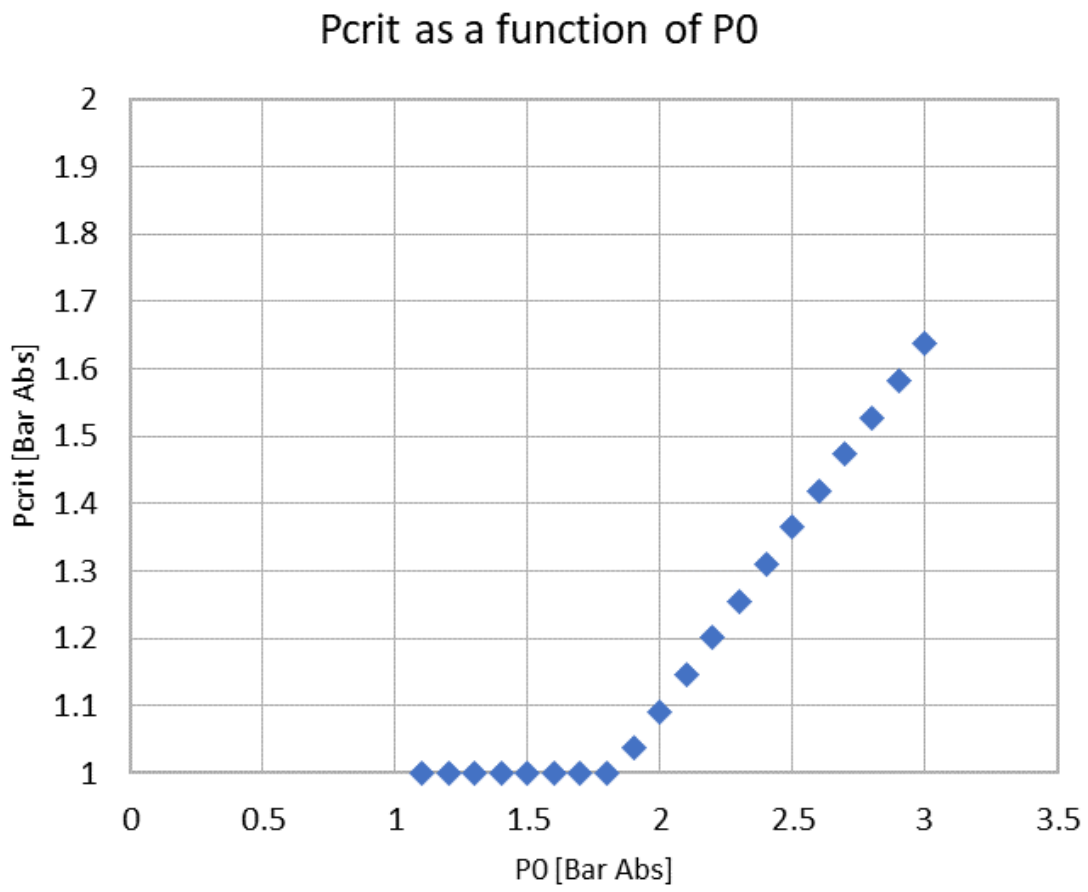

pressure drop at 2 Bar gauge blast pressure - roughly 1/3 of the available blast energy being wasted.

Figure 5: Variation of Pcrit with P0 when discharging to atmospheric pressure. Assumed ratio of specific heats = 1.3

2.4.3 The De
Laval Nozzle

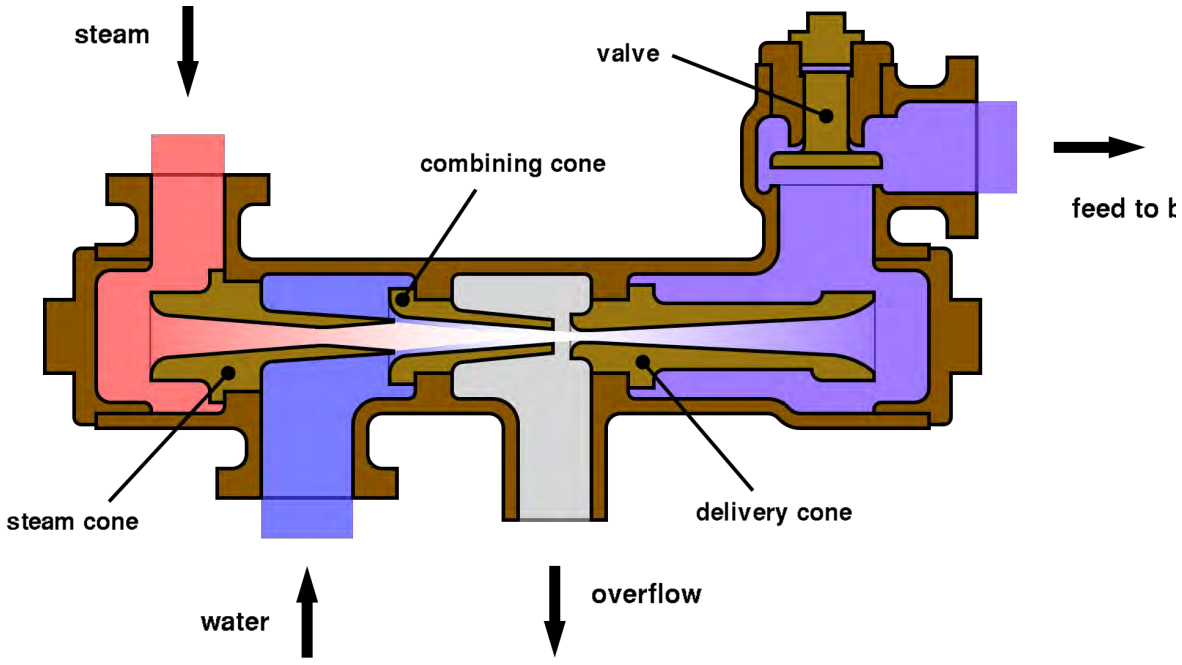

(Convergent - Divergent)

For pressure drops greater than 12 psi, a nozzle can be designed to convert the enthalpy drop from P_c to P_2 (Figure 4) into useful velocity energy. It requires the addition of a divergent section after the throat. Such a nozzle is shown in the steam cone of an injector in Figure 6.

Figure 6: Cross section through steam injector, showing De Laval nozzle form in steam cone.

The first problem is that if a pressure drop less than the critical value is used, the diverging section of a De Laval nozzle will decelerate the flow from its maximum velocity at the throat; the equations given in Section 2.3 would apply with the exit area being the relevant area. The second problem is that even when the pressure drop exceeds the critical value, a De Laval nozzle of a given geometry is only suitable for one value of pressure ratio, as given by equation 12.59 from Ref. 4.5 :

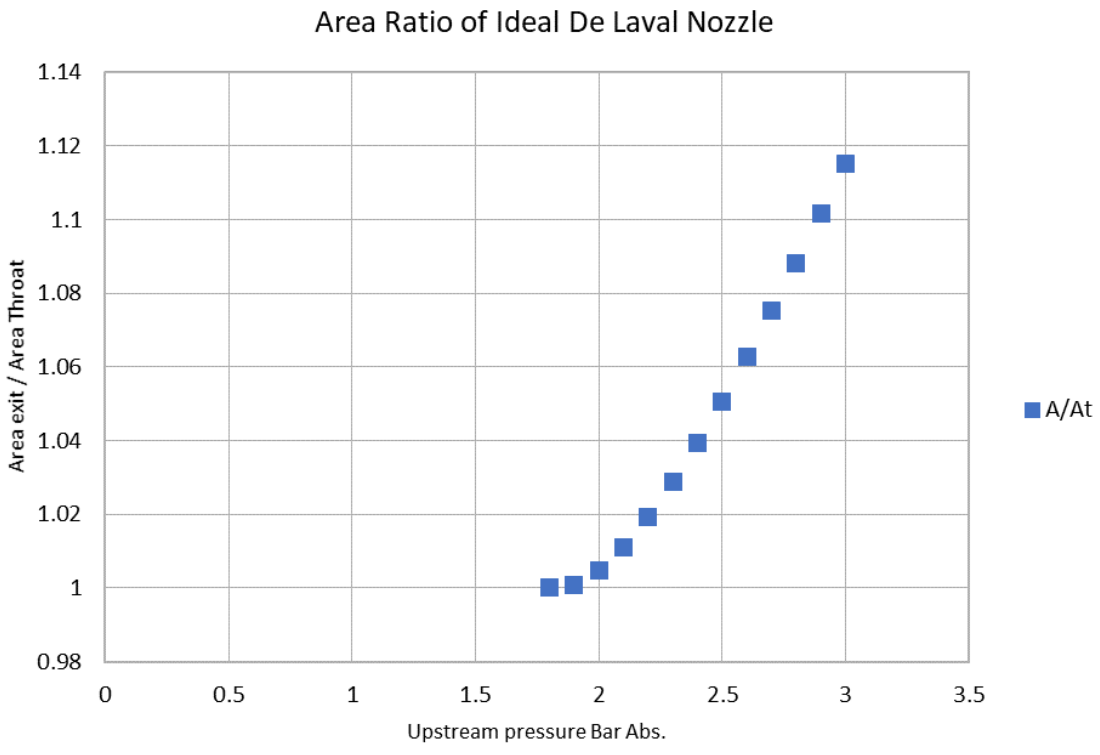

Figure 7: Area ratio of De Laval nozzle to suit a given upstream pressure. Assumed ratio of specific heats = 1.3 and discharge pressure 1 Bar Abs.

$$(\frac{A_t}{A})^2 \times \frac{2}{(\gamma+1)}^{\frac{(\gamma+1)}{(\gamma-1)}} = \frac{2}{(\gamma-1)} \times [(\frac{p}{p_0})^{\frac{2}{\gamma}} - (\frac{p}{p_0})^{(\frac{(\gamma+1)}{\gamma})}]$$

Where:

A_t = Area of nozzle throat [m2]

A = Area of nozzle outlet [m2]

p = Total pressure at nozzle outlet [Bar]

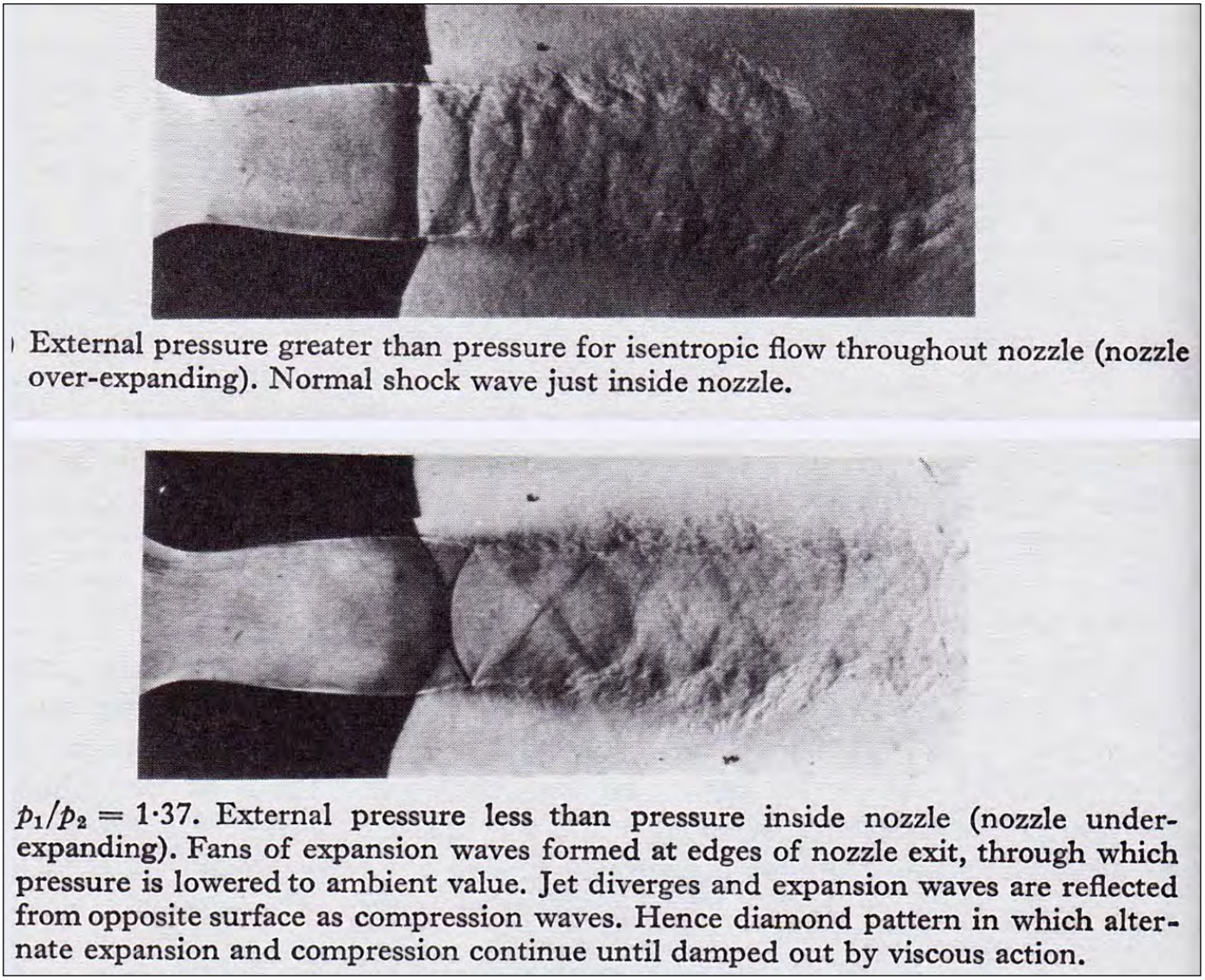

External pressure greater than pressure for isentropic flow throughout nozzle (nozzle over-expanding). Normal shock wave just inside nozzle.

$p_1/p_2 = 1{\cdot}37$. External pressure less than pressure inside nozzle (nozzle under-expanding). Fans of expansion waves formed at edges of nozzle exit, through which pressure is lowered to ambient value. Jet diverges and expansion waves are reflected from opposite surface as compression waves. Hence diamond pattern in which alternate expansion and compression continue until damped out by viscous action.

p_0 = Total (stagnation) pressure at nozzle inlet [Bar]

γ = Ratio of specific heats [Dimensionless]

Figure 7 shows that there is a fixed relationship between upstream pressure and the area ratio of a correctly designed De Laval nozzle for a given fluid and exit conditions. As an example, Chris Corney sent me a copy of Ref. 4.4 describing the "Selkirk" tests and resulting front end arrangement. The Selkirk front end included a blast pipe with a De Laval nozzle with an exit area / throat area of approximately 1.1, suggesting the Selkirk designers were designing for pressures around 2.9 Bar exhaust pressure. In the case of the steam injector illustrated in Figure 6, it works over a relatively narrow band of pressures, so

would be designed to give reasonable matching in the middle of that range. Those with footplate experience will know that injectors have a limited pressure range for dry operation and sometimes two units of different ranges are fitted; now you know why that is so.

Conversely, the pressure drop in a blast pipe is varying widely at every exhaust beat, and with the engine duty. At pressures not coinciding to that for the area ratio, the nozzle will be "over expanding" or "under expanding", and in both cases flow deceleration from supersonic to sub-sonic will be as a shock wave. A shock wave is not an isentropic process, and as in Figure 4, an entropy increase and consequent reduction in enthalpy drop will result. In the case of the De Laval nozzle the entropy increase would be

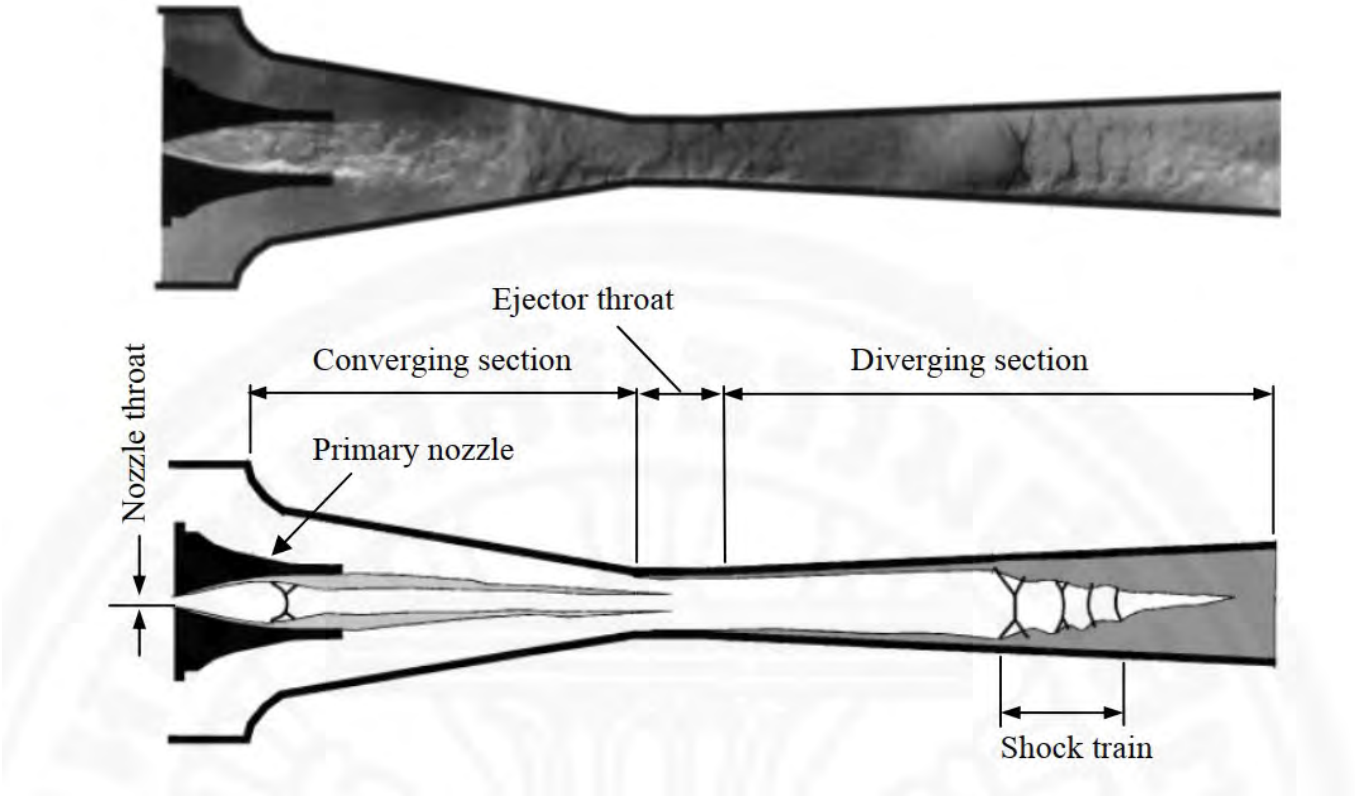

less than the case illustrated in Figure 4. Figure 8 shows a De Laval nozzle in both over and under expanding modes, (that is each side of the optimum pressure ratio for the given nozzle area ratio) and illustrates the presence of shock waves.

While it would in theory be possible to calculate the full enthalpy - entropy diagram for the under and over expanding cases, the process would be complex and lengthy and is more than I can reasonably cover here.

Figure 8: De Laval nozzles operating in the over expanding (top) and under expanding (bottom) modes. From Ref. 4.5 .

Fortunately, the change in optimum area ratio across the range of pressure drops in blast pipes is relatively small, so one might argue it is not a major issue, if the nozzle were designed for the middle of the operating range. However, even at the design point, there will still be a shock transition from supersonic to sub-sonic flow as soon as the steam starts entraining low velocity gas.

Figure 9 (For which I thank Chris Corney) shows the flow pattern in a supersonic jet pump. This design is for much more extreme inlet pressures than blast pipes; the primary nozzle area ratio being around 25 to 1, which is way beyond the range illustrated in Figure 7. Nevertheless, the patterns give some insight into blast pipe supersonic behaviour. Figure 9 shows:

- A plane shock within the primary nozzle (indicating over expansion) which initiates flow separation

in the nozzle which persists until just beyond the mixing section throat.

- Supersonic flow through to the diverging section where a train of shock waves marks the transition back to sub-sonic flow. In a blast pipe operating at much lower pressures and hence velocities, the shock train would occur much nearer the primary nozzle.

Figure 9: Schlieren photograph of a complete supersonic jet pump

2.4.4 Supersonic Flow - A Recommendation

The theory set out above shows that when supersonic conditions are reached at the blast pipe, there must be a shock wave or series of shock waves as flow returns to sub-sonic at some point in the front end - resulting in significant losses. For that reason, the authors advice would be to avoid supersonic conditions as much as possible by optimising the sub-sonic performance, which results in larger blast nozzles for a given duty, hence lower velocities and hence extends the sub-sonic performance envelope.

My own opinion is that I would not expect any significant benefit from designing front ends with De Laval nozzles and in support of that view, I offer quotes from two references:

> "The use of convergent-divergent nozzles is recommended, provided the primary pressure, p_{t1}, is sufficiently high to enable it to operate correctly. **However, the divergence may present problems if the primary pressure is liable to fluctuate or drop; convergent-only nozzles should be used in these cases.**" From Ref. 4.6

> "The ratio of exit area to throat area for nozzle A (a De Laval nozzle) is much greater than the theoretical ideal, being 4 instead of a “correct” value of rather less than 2 for the pressure ratios involved, but a progressive shortening of the nozzle resulting in a reduction of exit area (the position of the nozzle outlet relative to the combining tube being, of course, kept constant) indicated that over-expansion had no advantages, **and forcing nozzle B which was used for nearly all subsequent experiments, was designed to give no expansion (plain orifice) in the nozzle beyond the throat, and proved very successful**" From Ref. 4.7

In both cases the highlighting is mine.

A further point for thought. An orifice plate style of nozzle (See Fig. 4 Right hand side in the article in ASTT Newsletter 16) tends not to give a well defined transition to sonic behaviour; rather than a plane shock forming on the walls of a nozzle, oblique shock waves form on the edges of the orifice. This gives a smaller increase in pressure drop for a given flow rate above the critical, which seems to be ideal for a locomotive blast pipe.

2.5 Crossing the Saturation Line

The previous sections have illustrated how a real nozzle expands steam with a drop in pressure, drop in enthalpy and an increase in entropy. However, if the process crosses the saturation line it can affect the

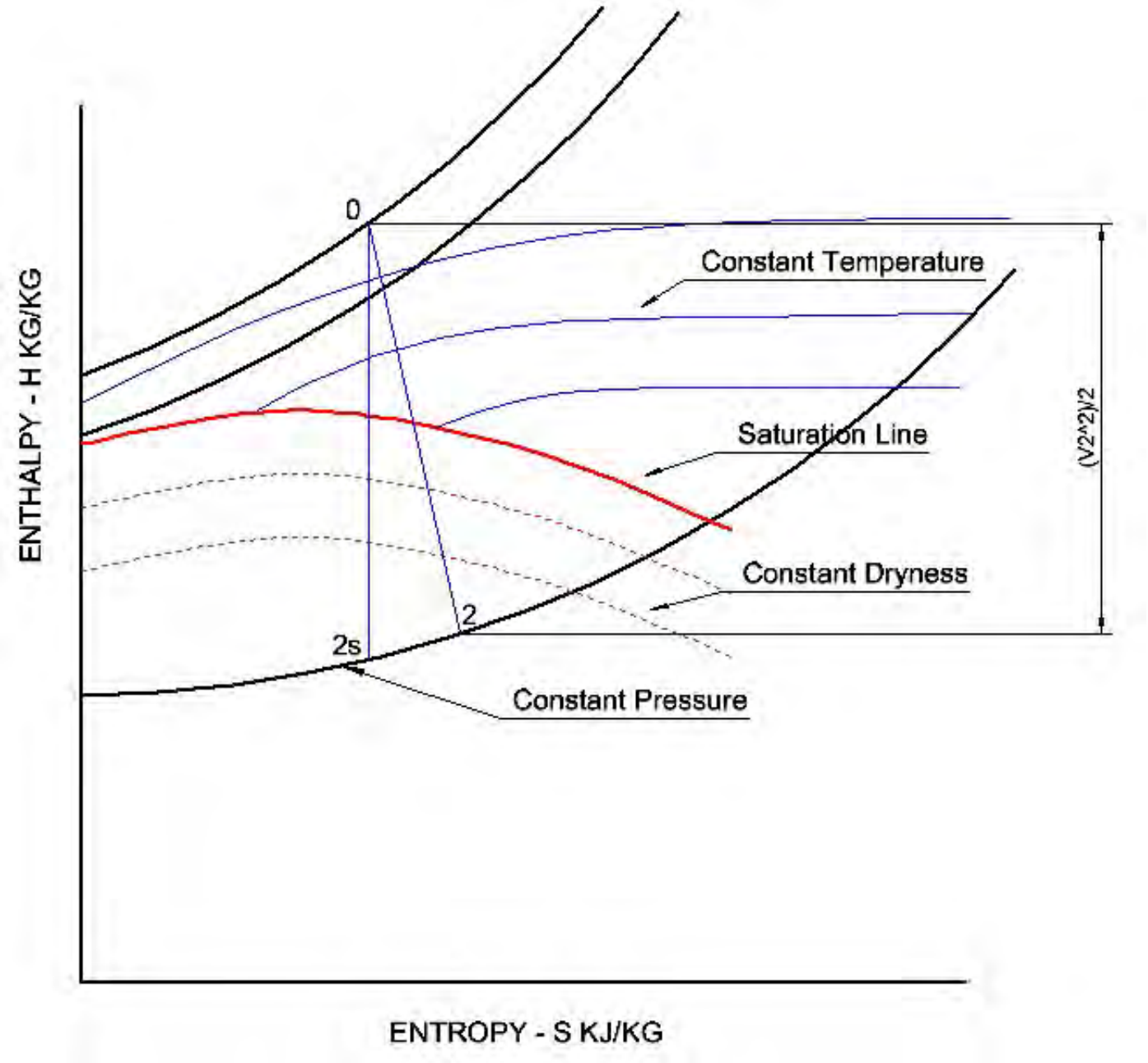

available enthalpy drop for conversion into velocity energy.

2.5.1 Expansion Starting in the Wet Steam Region

If the start point for the process lays below the saturation line (quite possible in a saturated locomotive), the relevant enthalpy drop will be found by reference to the wet steam curves on the enthalpy - entropy diagram, generally as described in Section 2.3 . When calculating mass flow, the density will be that of wet steam which is approximately:

$$\rho_w = \rho_s \times drynessfraction$$

Where:

ρ_w = Density of wet steam [kg/m^3]

ρ_s = Density of saturated steam [kg/m^3]

Dryness fraction is as read from the enthalpy entropy diagram.

2.5.2 Expansion Starting in the Superheated Region

If the process starts in the superheated region, as shown in Figure 10, the steam continues to expand as a vapour (no wetness) into the wet region. This happens because the process of condensation involves transfer of latent heat and therefore needs time and nucleation sites to initiate condensation. Therefore, for short time periods (longer than the transit time through a nozzle) the steam can exist in a meta-stable superheated state. That being so, the velocity calculations as outlined in Section 2.3 or 2.4 apply BUT the enthalpy drop is calculated from the gas law equations, using the specific heat ratio 1.3 for superheated steam.

Figure 10: Nozzle enthalpy drop from superheated to the wet steam region

The enthalpy drop between 0 and 2 would be:

$$h_0 - h_2 = \frac{\gamma}{1-\gamma}\frac{p_0}{\rho_2}\left[\left(\frac{p_2}{p_0}\right)^{\frac{\gamma-1}{\gamma}} - 1\right]$$

Where:

$$\rho_2 = \frac{\rho_0}{\left(\frac{p_0}{p_2}\right)^{1/\gamma}}$$

ρ_2 = Density of exit steam [m^3/kg]

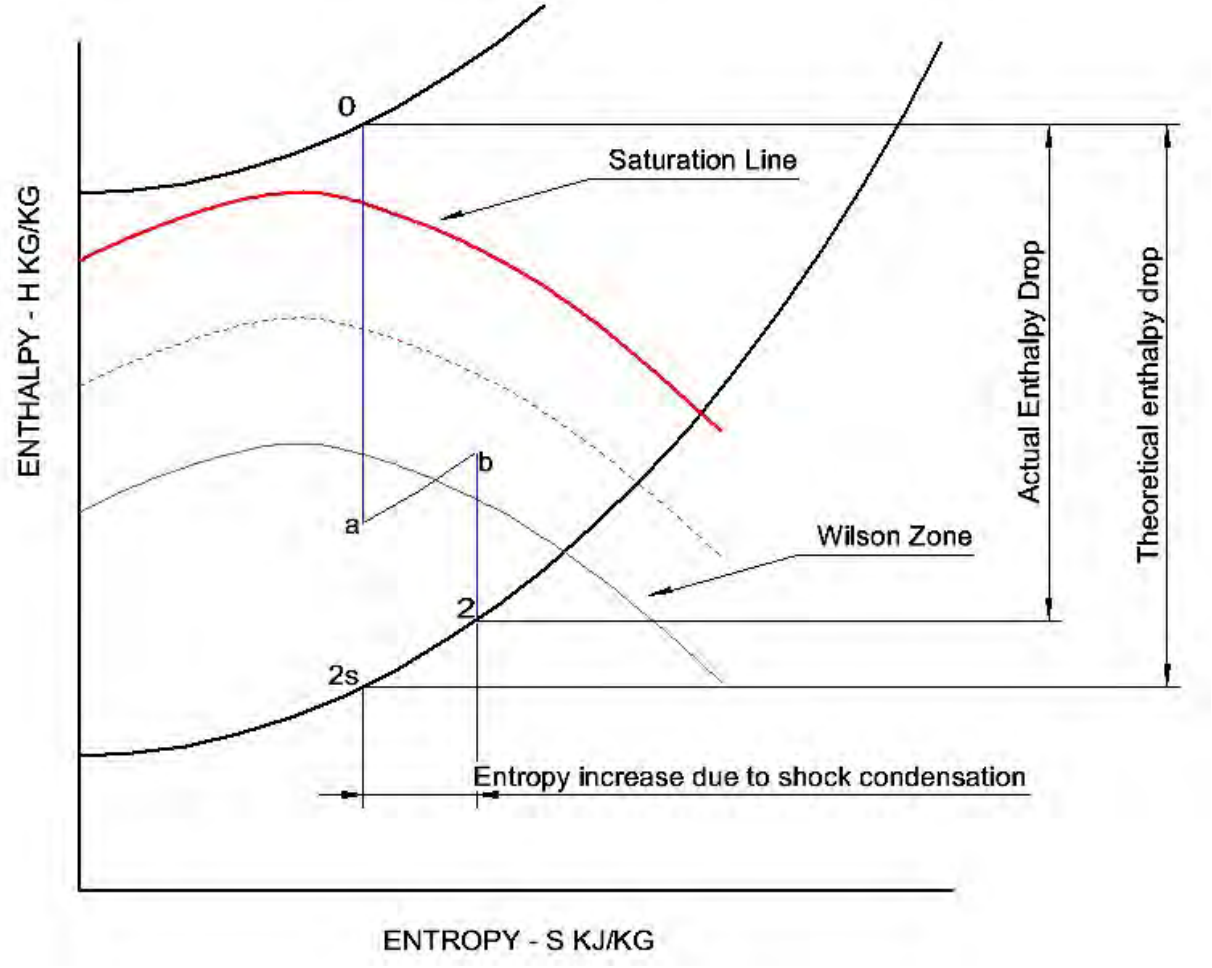

Figure 11: Loss of energy due to shock condensation in wet steam region.

ρ_0 = Density, read from steam tables at p_0 & t_0 [m^3/kg]

p_0 = Pressure at point 0 in Figure 10 [Bar Abs]

p_2 = Pressure at point 2 in Figure 10 [Bar Abs]

The mass flow will be:

$$M = \rho_c V_2 C_c A$$

Once the steam leaves the nozzle, it will be surrounded by and entraining hot flue gas, so condensation would not subsequently take place due to the heat transfer into the steam.

The above method gives a somewhat higher mass flow and velocity for a given pressure drop compared to taking enthalpy values from the wet region of the enthalpy - entropy diagram.

2.5.3 Instability of the Meta Stable State

Research in the 1960's found that the meta-stable state can only be pushed so far; if the process drops below some 96% dryness condensation will take place very rapidly. The region just under the 96% dryness line is sometimes known as the Wilson line or zone and is important in steam turbine technology.

Once the process crosses the Wilson zone, rapid condensation to convert the meta stable superheated steam to wet steam generates a shock loss that will increase the entropy and hence reduce the available enthalpy drop - thus reducing velocity produced. This would normally happen in the diverging section of a convergent divergent nozzle but can also take place immediately downstream of a plain convergent nozzle.

Figure 11 shows the pattern of enthalpy change when crossing the Wilson zone. A normal isentropic expansion (assuming a perfect nozzle) could be sustained to from 0 to point a as described in 2.5.2 . Then sudden condensation takes place which may follow a constant pressure line or increase pressure (sources differ on this point) to point b. Subsequent expansion takes place isentropically according to the wet steam data on the enthalpy - entropy diagram. Figure 11 shows how the resulting enthalpy drop would be less than a fully isentropic expansion.

This effect is unlikely to be seen on a superheated engine, so holds little interest for future designs. However, it may affect the interpretation of historical data on saturated engines. As an example, an expansion of saturated steam from 1 Bar gauge to atmospheric pressure is about the maximum pressure drop that could be sustained without crossing the Wilson line. More information can be found about the Wilson line in Ref. 4.8 .

3. NOZZLES - A SUMMARY

Porta's theory (Ref. 4.1) starts with an assumption of nozzle velocity, but says nothing about how to calculate the required steam conditions to achieve the required velocity. Porta does include a factor which is equivalent to an assumed C_v factor of 0.99, which is used as an uplift on the calculated required nozzle velocity.

Koopmans' theory as outlined in Ref. 4.2 takes no account of nozzle efficiency, contraction coefficient (vena contracta effect) or possible complications from sonic flow or expansion below the saturation line.

In my own limited reading of locomotive front end theory I have not seen a detailed summary of nozzle

calculations arranged for the case of a blast pipe, although there is plenty of relevant material around in support of steam turbine design. I hope this article has pushed understanding of blast pipes further forward.

Next time, I shall deal with the question of what design conditions should be specified for a locomotive front end, which I hope will provide some relief after this equation heavy episode!

4. REFERENCES

4.1 Porta, L.D. - "Theory of the Lempor Ejector as Applied to Produce Draught in Steam Locomotives" http://www.trainweb.org/tusp/lempor/lempor_theory.pdf (1974)

4.2 Koopmans J.J.G. - "On the Calculation of Steam Locomotive Front-End Performance" Publ. Jnl of Stephenson Locomotive Society September/October 2017- No. 907, Volume 93 p. 201 also available at: https://www.researchgate.net/publication/320756980_On_the_calculation_of_steam_locomotive_front-end_performance

4.3 Young. E.G. - "A Study Of The Locomotive Frontend, Including Tests Of A Front-End Model" Bulletin 256 University of Illinois May 30th 1933 also available at: **https://www.ideals.illinois.edu/handle/2142/4435 and https://www.ideals.illinois.edu/handle/2142/4484**

4.4 Collins, W.F. "Standing Locomotive Tests" Railway Mechanical Engineer Feb 1941 pp 57-59 & March 1941 pp 96-100 (1941)

4.5 Massey B.S. "Mechanics of Fluids" 3rd Edition Publ.Van Nostrand Rheinhold 1968

4.6 Anon - "Ejectors and Jet Pumps - Computer prgram for design and performance for compressible gas flow", Publ. ESDU Intl. Item No. 92042, (Dec. 1992)

4.7 Kastner, L.J., Spooner, J.R. "An investigation of the performance and design of the air ejector employing low pressure air as the driving fluid" Proc. I. Mech. E. June 1950 (1950)

4.8 Chaplin R.A. "Thermal Power Plants – Vol. Iii - Steam Turbine Operational Aspects" http://www.eolss.net/Sample-Chapters/C08/E3-10-03-05.pdf

INTERNAL AERODYNAMICS OF A MERCHANT NAVY PACIFIC

By Steve Rapley, with Colin Dixon, Adam Keir, Annysa Mohamad-Mansor, Aditya Ramesh and Alfredo Stock

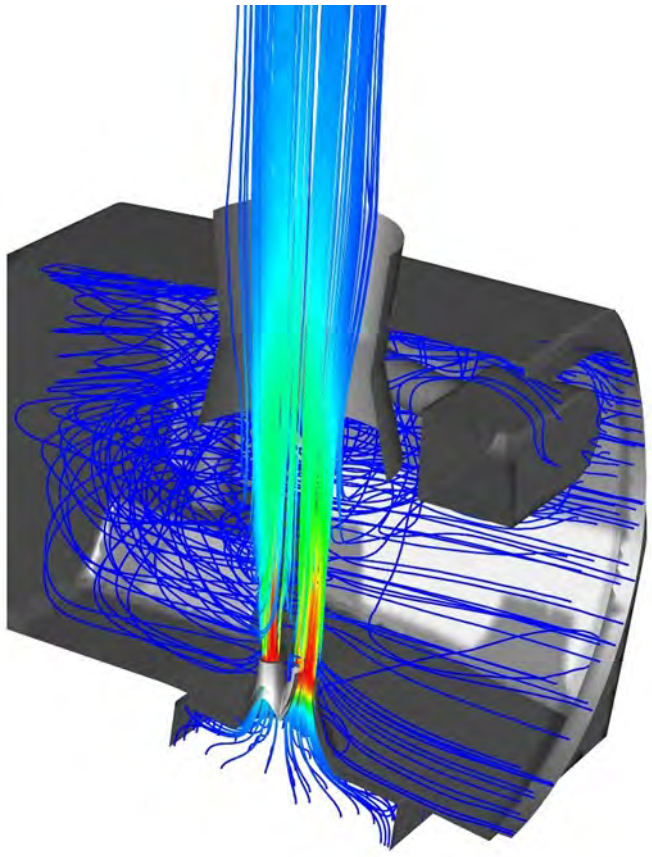

1. Background & Introduction

As discussed in a previous newsletter, the General Steam Navigation CIC are custodians of BR Rebuilt Merchant Navy Pacific locomotive 35011 General Steam Navigation, the plan for which is to return it to original design condition, complete with the original air smoothed casing, chain driven valve gear, quasi-hexagonal smokebox, and Bulleid-Lemaître exhaust. I am the Chief Mechanical Engineer for the General Steam Navigation CIC, and as a way of drumming up interest in our project as well as improving the performance of the locomotive, I approached contacts I have at Loughborough University about conducting some CFD studies of the external aerodynamics of a Merchant Navy, to see if we could improve the issue of drifting smoke with the design. After conversations with Professor Versteeg, this idea grew into two projects, looking at the internal and external aerodynamics of a Merchant Navy, using Computational Fluid Dynamics (CFD) to place our locomotive in a virtual wind tunnel. Our goal with these projects was to explore (1) conditions in the smokebox and (2) the external exhaust clearance, with the possibility of making improvements on the design. In this article I'll give a condensed version of the report from the internal aerodynamics study conducted by a group of 4th year Mechanical Engineering students at Loughborough University, under the supervision of Professors Versteeg & Malalasekera.

Smokebox & locomotive exhaust design is a problem which plagued all steam locomotive designers, with many engineers attempting to develop the optimum exhaust for their locomotive. On his pacific locomotives OVS Bulleid implemented what I'll refer to as a Bulleid-Lemaître exhaust; it encapsulates many of the features of the original Lemaitre design, with a Bulleid twist. Whilst I am an obvious fan and proponent of the work of Bulleid, I can also see where some of his ideas fell short of either his vision or their potential, whilst others were hampered by the conditions he was designing the locomotive under.

The exhaust applied to his pacific locomotives is a product of some of these shortcomings; compared to contemporaneous locomotives the total steam nozzle exit area is rather undersized, and the fact the same design was applied to both the Merchant Navy & Light Pacifics with no change may suggest it wasn't fully designed for either. Compared to the original Lemaitre design, the nozzles are also too far from the base of the chimney, with an effective choke 7 inches below the real choke. Despite all this, on testing it was shown to produce a strong draught, producing 10-20% more flow through the boiler than the design fitted to the rebuilt design.

The aim of the study was to evaluate and compare various exhaust and nozzle design with regards to the original design manufactured pre-1959 using CFD simulations carried out in StarCCM+, a commercial computational fluid dynamics software. The report highlights the general model setup, which includes mesh refinement, boundary conditions, and comparisons to the Rugby test data [1]. Individual group members studied various models which may have different exhaust or nozzle geometries. To conclude, the obtained results will be compared to the original design and provide an analysis as to which design proves to be the most efficient. The aim of this project is to simulate various locomotive steam box designs and compare these to the original design. This will provide a performance comparison and indicate how the original design can improve. The validation test case used to verify the model is data from tests carried out at the Rugby Locomotive Testing Station in the early 1950s, detailed in [1].

In the following sections, italicised text are my thoughts or comments on the students work.

2. Basic Simulation

The objective of the initial group simulation was to produce a well-established baseline simulation, that the students could use to develop a methodology for use in their later individual tasks. By comparing against test data from the Performance & Efficiency report, it was hoped that a methodology could be arrived at that was consistent for the two different designs present. Unfortunately, for the project run during academic year 20/21 due to some early missteps the students ran out of time in the initial phase of the project to perform validations against both designs, and so only validated against the Bulleid-Lemaître design.

The CFD problem is to accurately model the fluid behaviour in the smokebox/exhaust region of the locomotive, in such a way that resembles the previously mentioned validation test case as closely as possible. The fluid interaction consists of high velocity, high pressure jets of steam flowing out of nozzles, entraining smoke through an exhaust.

In assessing the geometry for modelling purposes, several key assumptions have been made in attempt to replicate the condition of the test plan that was carried out in Rugby whilst aiming for reduced computational time and reduced complexity in modelling. In this project, the geometry was focused upon modelling the conditions inside smokebox rather than the entire locomotive, to capture the exhaust performance.

3. Modelling Assumptions and Material Selections

Heat dissipation from walls, pipes and flows from steam and air was assumed to be negligible in this case. When steam enters the smokebox, the steam may cool and condense but this was also assumed to be negligible. In selecting materials, smoke was modelled as air, whilst the steam was modelled as being

chemically pure (H_2O). The multi-component gas model was chosen to simulate air and steam as non-reacting species, since it allows the user to specify the proportion of the reactants and because the problem deals with miscible gases, whilst the ideal gas equation was chosen to be used across all the group's simulations. External factors like wind were ignored in order to replicate the conditions at the stationary testing facility where the validation data was collected [1], and because any performance improvements achieved under stationary conditions should carry over to moving conditions.

Simulations were conducted in a steady state in order to reduce computational time. From the various Reynolds-averaged Navier Stokes turbulence (RANS) turbulence models available in Star-CCM+, the realizable K-Epsilon turbulence model was chosen since it produced the most desirable results. It was arrived at after eliminating the rest of the turbulence models through trial and error.

3.1 Boundary Conditions

3.2 Boundaries and Types

Figure 1 shows the inlet and outlet boundaries labelled on the half model. The outlet (shaded orange) was set as a pressure outlet so that its pressure could be set to atmospheric pressure. The air inlet (shaded light brown) was set as a mass flow inlet to allow the air flow rate to be easily set and adjusted. The steam inlet (purple) was set as a pressure inlet, as this was found to be better for convergence (following experimentation by the group and advice from the industrial contact). The symmetry plane was set as a symmetry plane, with the remaining surfaces set as walls.

Figure 1: Geometry & Boundary Conditions

3.3 Flow Rates

Flow rates were calculated using data in the Performance & Efficiency Report [3], so that comparisons between the output of the simulation and validation data would be appropriate. There is data in [3] for three types of coal – Blidworth, Bedwas, and South Kirby – each with a different calorific value giving slightly different performance. It was decided to use Blidworth coal data to calculate flow rates, as there was only Blidworth coal data available to calculate air inlet temperatures.

The top left quadrant of graph 18 (in [3]) was used to calculate inlet flow rates. First, three steam flow rates were selected: 14,000, 20,000, and 28,000 lbm/hr. By converting units, these gave three "Feed Water Evaporated" values. The trendline of "Gas Flow" vs "Feed Water Evaporated" was used to find corresponding "Gas Flow" values, which were used as the air inlet flow rates: 27,000, 39,600, and 52,200 lbm/hr (graph 17 indicates that "Gas Flow" and air flow are closely linked). As the simulation was a half model with a symmetry plane, these flow rates were halved when inputted.

3.4 Temperatures

Air inlet temperatures were calculated using graph 3 (in [3]) to find the coal rate for each steam flow rate. These coal rates were used as inputs to graph 10 to find temperatures at the boiler exit at the exit of large tubes and small tubes. For each coal rate, an area-weighted-average boiler exit temperature, using boiler tube dimensions given in [3], was found. Steam inlet temperatures were taken from 'blastpipe temperature' (for Blidworth coal) on graph 11. An ambient temperature of 300K was used for the outlet.

3.5 Turbulence

The RNG K-epsilon turbulence model was used in the simulations, adopting an 'intensity + length' scale method. This turbulence model is the most appropriate for complex geometry.

3.6 Mesh design

A polyhedral mesh with a prism layer mesher was used for all models, with a base size of 0.1m. The polyhedral mesh is appropriate for complex geometries, but at a significantly reduced cell count, relative to a tetrahedral mesh. [4] It was key that the minimum number of cells which allowed a good quality solution were used. This reduced computing power required to complete simulations, and by extension, the amount of time required to complete iterations. Using a half geometry, the mesh cell count was further reduced, by around half, again allowing for faster iterations, without sacrificing the legitimacy of the solution.

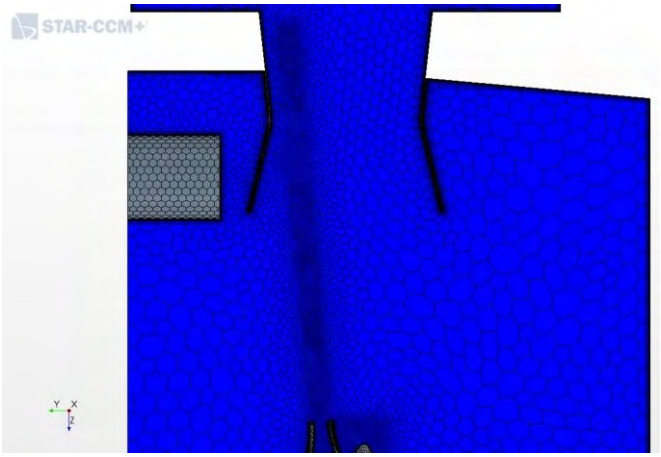

Figure 2: Mesh at symmetry plane

Based on my professional CFD experience simulating single nozzle ejectors at RRFCS, I recommended to the students to introduce a cylindrical mesh control volume, extending from the nozzle exit all the way to the diffuser exit, in order to focus the mesh in this region. Experience showed that this would keep the mesh size relatively small in this region. This is vital, as otherwise the primary flow can diffuse into the secondary flow by nature of the growth in mesh size, instead of via the shear between the two flows.

Figure 2 shows the mesh representation as seen on the symmetry plane. A well-defined mesh region can be seen projecting from the nozzle exit, extending towards the exit of the exhaust outlet. Each nozzle has its own identical extrusion. Targeted control volumes were utilised to employ a finer mesh in regions that had more detail or smaller geometries, such as around the nozzle cluster. Figure 3 illustrates this. The reducing cell size can be seen as the mesh approaches the nozzle cluster along the floor surface. The reduced cell size allows for good definition of the solid geometry of the nozzle cluster.

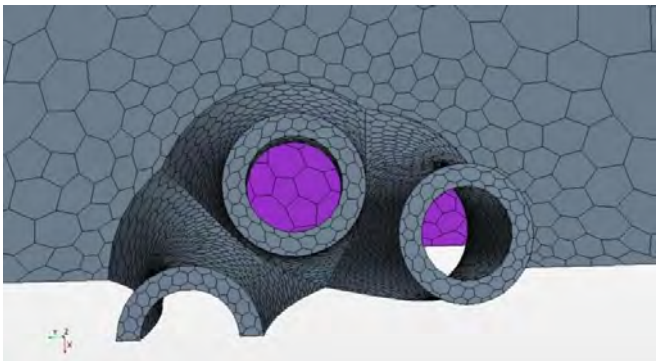

Figure 3: Nozzle Geometry Mesh Representation

A y^+ value of less than 1 was required on the nozzle inside and outside faces, and exhaust inside face. y^+ is a dimensionless metric that is used to describe how far into the boundary layer the near-wall cell resides; typically values of unity are targeted and can be achieved by having a significant amount of cells in the prism layers, in this case 21, and leaving the total thickness at an increased value. The increased number of prism layers, and, by extension, the significantly thinner first layer, then leads to a low y^+ value. Figure 4 depicts the y^+ values on the inside and outside faces of the nozzles. Whilst the steam flows through the centre of the nozzles, the flow entrained will be drawn up the exterior walls of the nozzle cluster. In other models, the global mesh was set to have an increased number (21) of prism layers, meaning that all walls had a y^+ value of less than one.

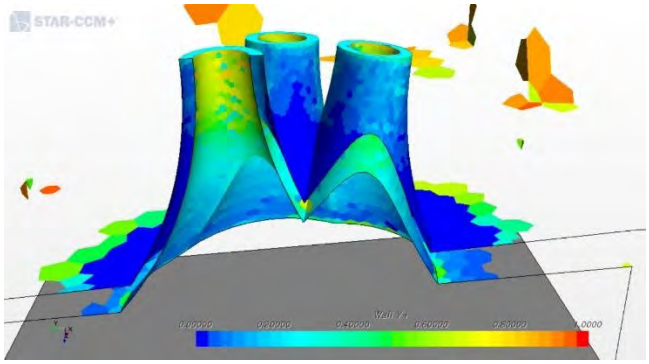

Figure 4: Wall Y+ Values on nozzle geometry

A second order discretisation scheme was used. This provides more accurate results, particularly in more complex flow, but can lead to worsened, or slower, convergence. For this reason, beginning the simulation under a first order scheme, then swapping to the second order scheme once the solution was partially converged was considered, but never executed. Residual targets for convergence were that all residuals were below 1e-3, with the energy residual below 1e-6. Other indicators were well developed flow which propagated deep into the cylindrical volume above the exhaust and remained stable within it, as seen by velocity scalar scenes, as well as observational checks that the flow was behaving as expected, illustrated by animated scenes with streamlines of the flow.

4. Simulation Results Analysis

Figure 5 illustrates the propagation of the flow through the smokebox into the exhaust. The flow does not follow the extruded nozzle mesh discussed previously, which runs parallel to the diverging exhaust wall towards the top of the geometry. Instead, the flow seems to straighten and tend towards the centre of the exhaust. For reference, the case depicted is the highest flow rate case. also demonstrates this; the flow can be seen converging towards the centre of the exhaust outlet. This suggests that the nozzles are not allowing the flow to make full use of the outlet cross-sectional area, reducing efficiency.

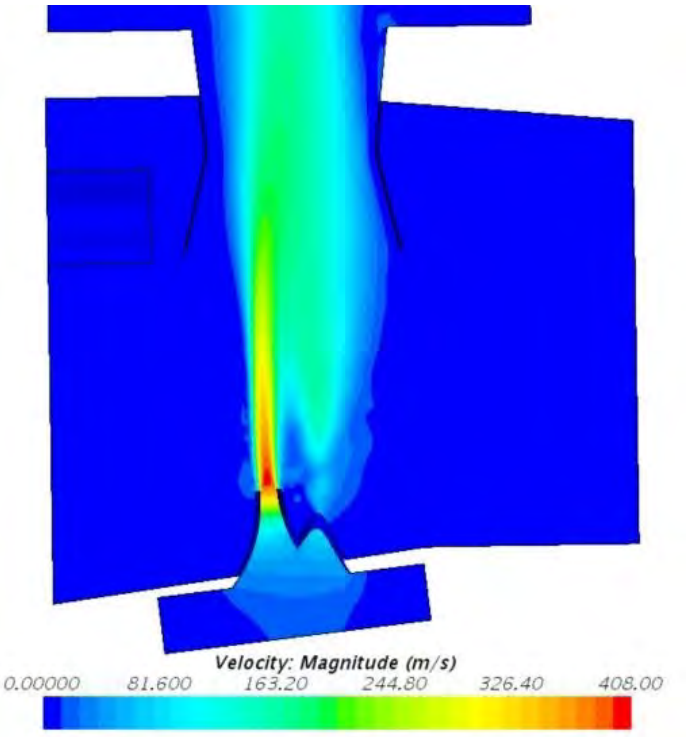

Figure 5: Contours of velocity magnitude on symmetry plane (Original Design)

It is important to validate CFD models with reliable test data to ensure that the model is accurate enough to be of use, and to determine the degree of confidence in the model. "Steam- Gas-Draught & Blast Pipe Pressure" graphs from the Performance & Efficiency report [1] were determined to be most useful for validation, as the data includes inputs and outputs (or measurements that are closely linked with these) of the simulation. Graph 18 was more relevant for comparison than graphs 20 and 22 because the type of coal used in graph 18 was used to calculate boundary conditions.

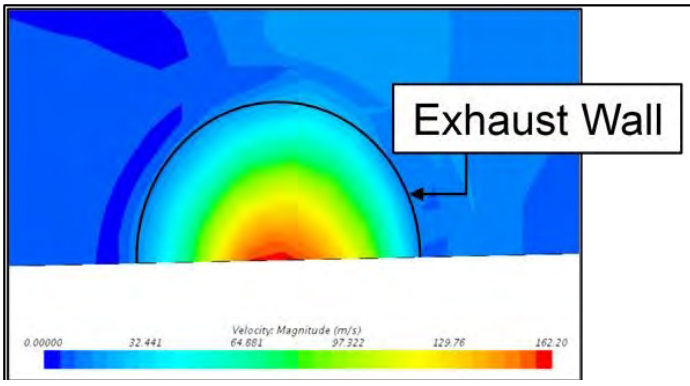

Figure 6: Velocity Magnitude Scalar Scene at Exhaust Outlet Plane

The first data comparison was with the top right

quadrant of Graph 18 (Figure 8) to check that the inputted steam inlet pressures (to obtain the target mass flow rates) matched the trend of the data. Target mass flows of 14000, 20000, and 28000 lb/hr gave "Feed Water Evaporated" values of 3.88, 5.56, and 7.78 lb/sec. The inlet pressures that gave these flows were 1.73, 3.71, and 7.20 psi – these were plotted against the "Pressure Below Blast Orifice" axis. There are a limited number of data points, but the data appears to fit the trend well. The test data trendline shows a higher gradient at smaller flow rates, which is reflected in the three data points taken from the simulation.

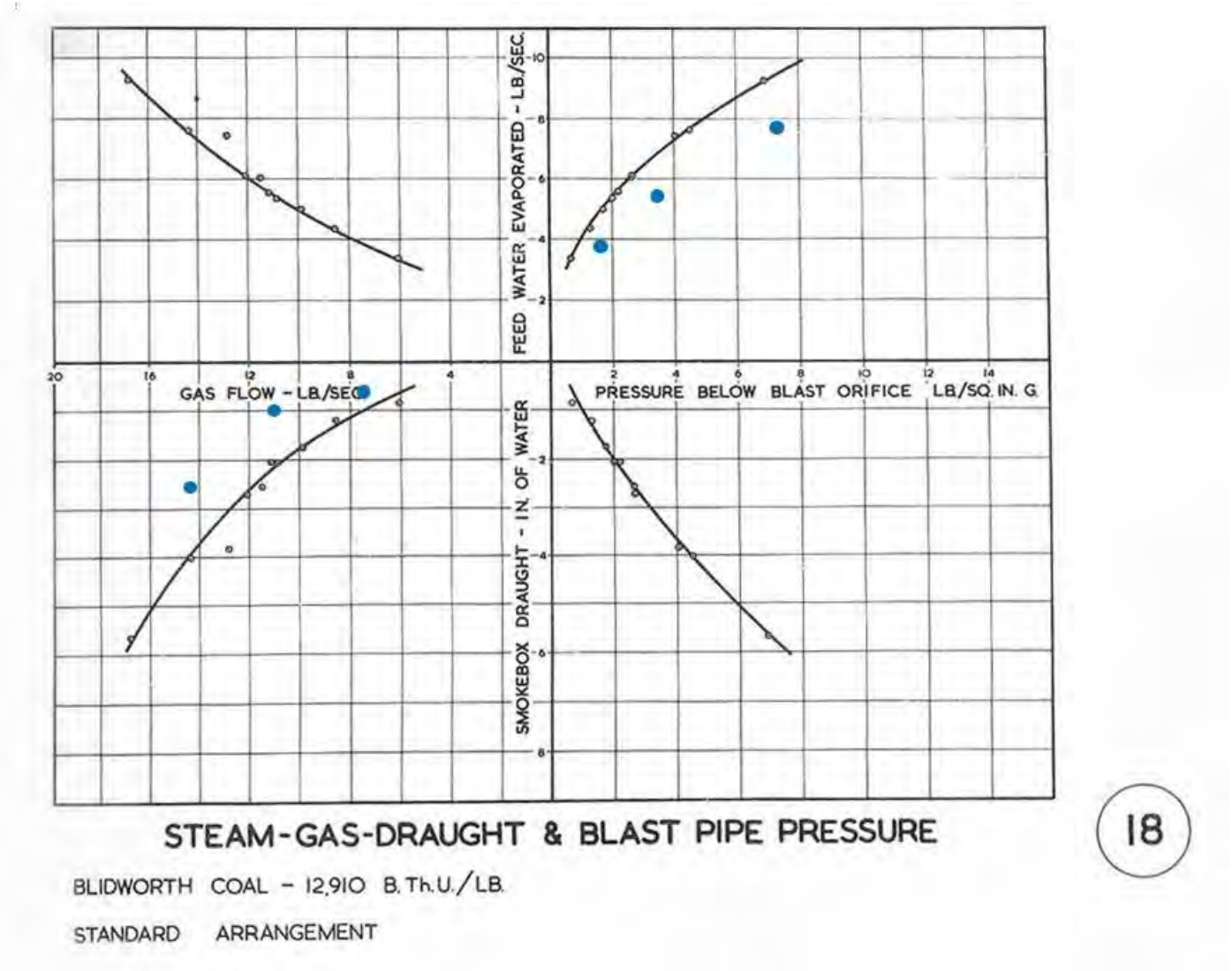

Figure 8: Graph 18 of Rugby Report [1] with Overlayed Data from Group Simulation

While they fit the general trend, the simulation data points are some distance from the trendline. This can be partly explained by the fact that "Feed Water Evaporated" does not exactly correspond to the steam flow rate through the nozzles, and "Pressure Below Blast Orifice" was almost certainly measured in a different place to the pressure inlet in the simulation. Simulation data was also compared with the bottom left quadrant of the graph (Figure 8). Air inlet flow rates of 7.5, 11, and 14.5 lb/sec were assumed to correspond to the "Gas Flow" axis, and values of "Smokebox Draught" were calculated for comparison with the test data trendline. "Smokebox Draught" refers to a pressure measured somewhere in the smokebox, away from the blast region. To obtain a comparable measurement from the simulations, a report was run to find the mass-flow-averaged pressure at the air inlet, and then the mass-flow-averaged

pressure at a plane section just above the exhaust was subtracted. The air inlet was chosen as a reasonable part to measure the initial smokebox pressure value, although other probe regions could have been used as there was not significant variation of pressure throughout the smokebox. The pressure above the exhaust was subtracted to account for the fact that, in the test, there was a gap between the exhaust top and the vent cylinder which was not modelled in the simulation. Therefore, the pressure drop though the modelled vent cylinder needed to be accounted for to compare like with like (pressure drop from smokebox to top of exhaust). This gave smokebox draught values of 0.606, 0.968, and 2.470 inches H_2O, which followed the trend of the test data (Figure 8). The fact that the points lie at a distance from the curve may be explained by differences between Gas Flow and air flow rate, differences between Smokebox Draught and the measurement taken from the simulation; and assumptions/ simplifications in modelling (e.g. geometry, calculation of boundary conditions). The fact that both sets of simulation data capture the trend of the test data provides further validation of the model. Following the validation of the original design group simulation, the group individually continued further work focusing on separate models with modifications in geometries. This way, the theory of other designs including Lempor exhaust and Giesl ejector as described in the literature can be tested against performance of the original design to measure the difference in efficiencies between model designs to reach appropriate conclusions for design improvement. The models used for the individual simulations were:

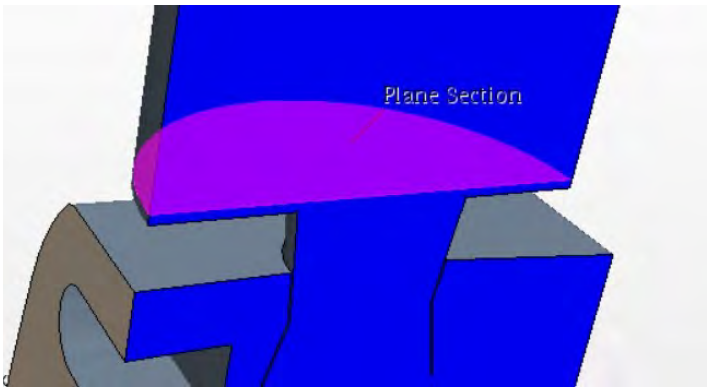

Figure 7: Plane section used in calculation of smoke-box draught

- Bulleid-Lemaître exhaust, where the nozzles point to the centre of area (COA).
- A 7-degree Lempor exhaust with 4.14° nozzles.
- A 6-degree Lempor exhaust with 4 nozzles. (I'm not presenting the section of the students report on the 6-degree Lempor with 4 nozzles, as based on the flow structures presented, I don't feel the results were fully converged.)
- A 7-degree Giesl ejector.
- A 5-degree Lempor exhaust.

I have some trepidation about presenting the results of the individual tasks; the more I look at the results, the less faith I have in them. As mentioned elsewhere, the students ran out of time to validate the methodology against a second data set, which reduced my confidence in the results presented in the following section. As will be shown, some of these results lie in the realm of "too good to be true", unless the methodology can be validated further. They do however highlight some of the difficulties of simulating the conditions in a locomotive smokebox.

5. Individual Tasks

5.1 Bulleid-Lemaître exhaust with COA Nozzles

Whilst I was working at RRFCS, we looked at running multiple ejectors in parallel, and then combining those ejectors into a multi-nozzle oblong ejector. This showed that the performance of the oblong ejector

could be brought in line with the multiple ejectors if the flow area at the diffuser exit per nozzle were maintained, bringing in a certain amount of symmetry. I hypothesized that the performance of the Bulleid -Lemaître exhaust could be similarly improved, or at least stabilised, by adjusting the nozzle angle so the nozzles are directed towards the centre of area of the segments of the exhaust, so at a point $\frac{r}{\sqrt{2}}$ *from the centre of the exhaust.*

Differences in flow profiles/results

Clear differences between the original design and original design with COA can be seen when analysing the velocity flow profiles. Figure 10 shows a comparison for the middle case (20,000lbs/hr steam), but these differences were consistent for each set of flow rates. The peak velocity decreased – from 213 to 202 m/s for 14'000 lb/hr steam, from 302 to 289 m/s for 20'000 lb/hr steam, and from 408 to 395 m/s for 28'000 lb/hr steam, as lower inlet pressures were needed to achieve the target mass flow rates. This may point to an improvement in the performance of the diffuser, which is supported by differences in how the flow interacts with it. With the COA nozzles, there is much less separation between the steam jet and exhaust wall than with the original nozzles, and the steam flow follows the path of the extruded cylindrical mesh refinement. This indicates better performance as flow separation from the exhaust wall inhibits pressure recovery across the diffuser. Figure 10 shows that the steam jets remain separate at the exhaust outlet, rather than converging as in the group simulation (Figure 5). There are also smaller regions of medium velocities surrounding the main steam jet; this may be due to the steam following the path of mesh refinement, meaning there is less numerical diffusion of the steam through the coarser mesh.

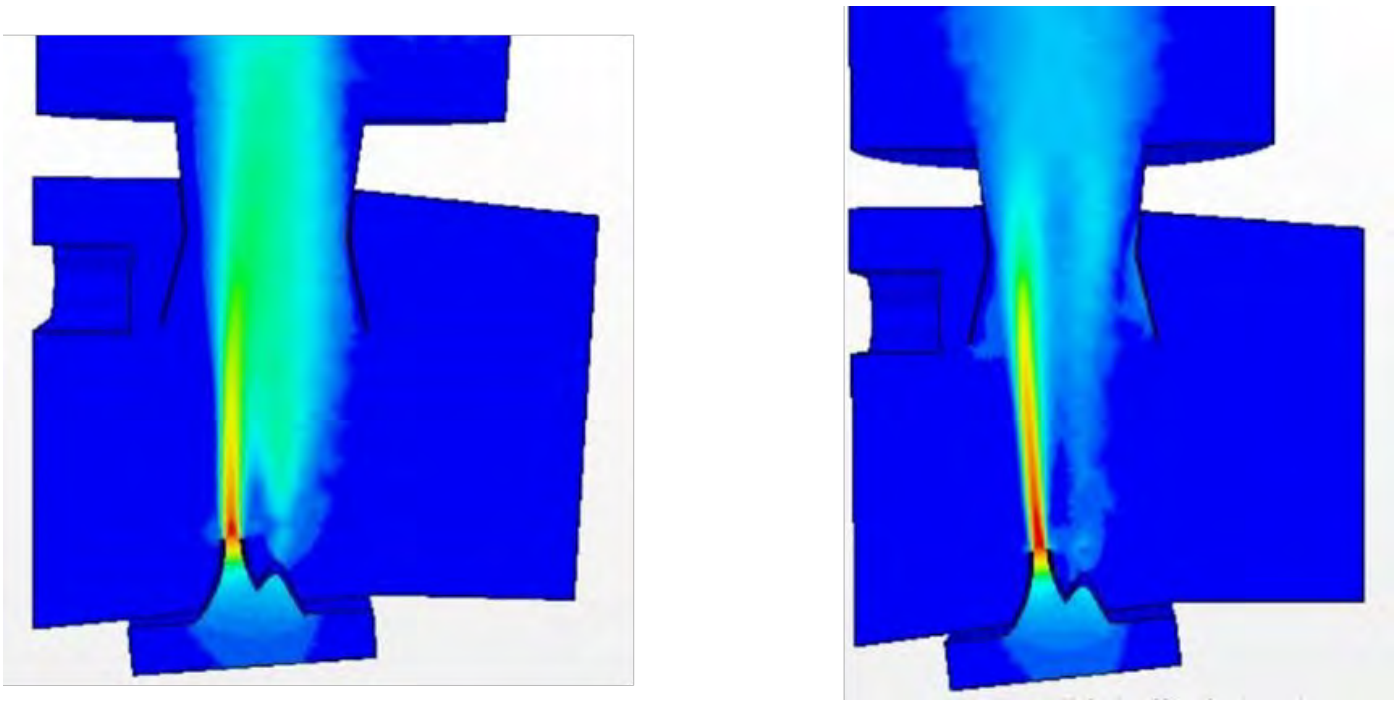

Figure 9: Velocity flow profile for original design (left) and original design with COA (right) for 20'000 lb/ hr steam

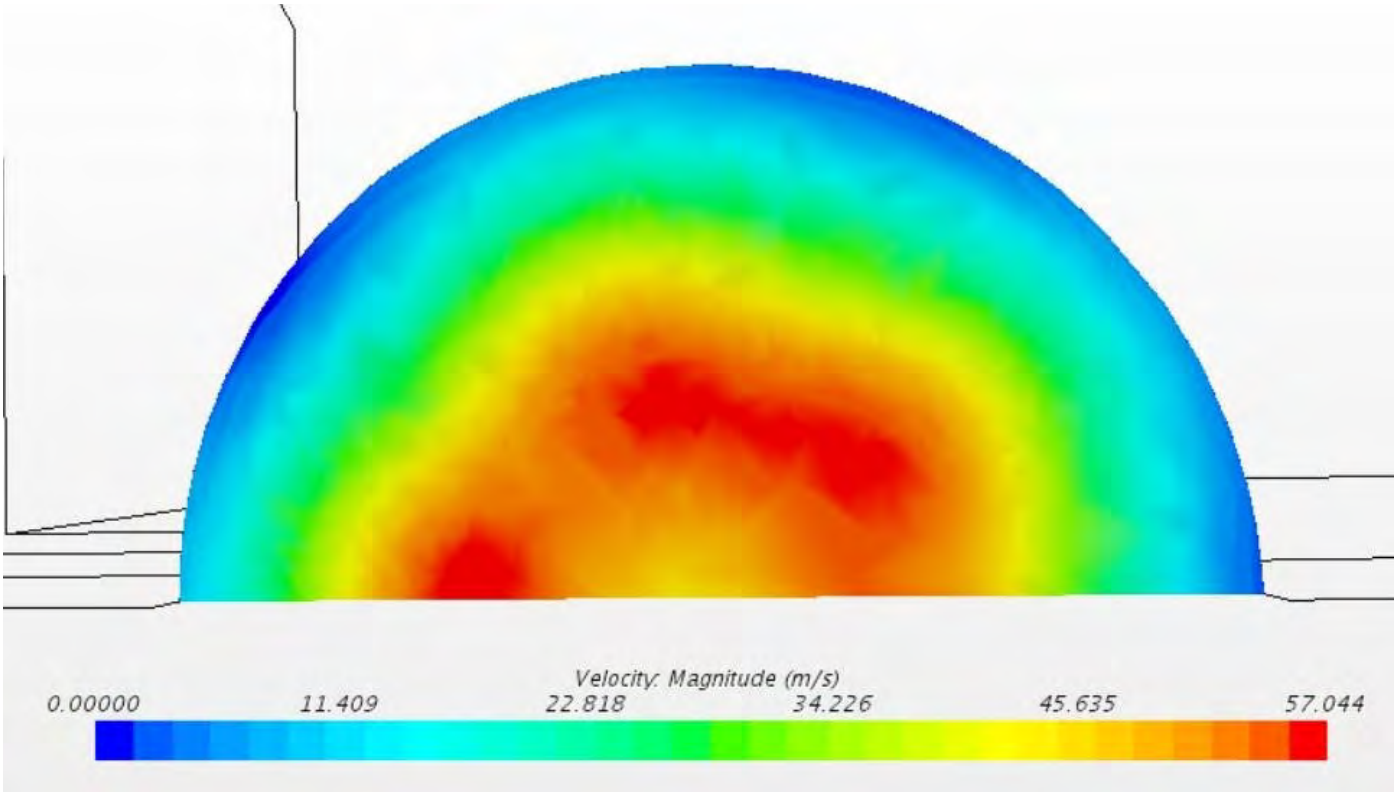

Figure 10: Velocity Magnitude at Exhaust Outlet Plane (20,000 lb/hr steam)

Performance indicators (smokebox draught and steam inlet pressure)

Smokebox draught values were found to be much larger than for the original design at each set of flow rates, suggesting improved performance. This pressure increased significantly considering that the angle of the nozzles was changed by a very small amount, however this could be explained by the difference in flow structure eliminating separation between the steam jets and exhaust wall.

Steam inlet pressures needed to produce the target mass flow rates all decreased slightly with the introduction of COA nozzles (see Figure 21 for values), indicating improved performance. The air inlet pressure monitor shows that it is varying through a range of 1090Pa to 1190Pa, so the simulation may not be as well converged as the group simulation, or there may be a tendency for transience in the solution that the steady-state cannot resolve.

5.2 7 Degree Lempor, 4.14 Degree Nozzles

The objective of this individual task is to analyse the 7° Lempor chimney with nozzle centre axes at 4.14° to the axis of the chimney centre geometry, again orienting the nozzles towards the centre of area of the 1/5th sectors of the exhaust. Relevant metrics remain steam inlet pressure and pressure difference. The purpose of this simulation is to provide data that can be fairly compared to the others, with the hope that an optimised design, or designs, can be identified. The boundary conditions shown in Figure 11 are consistent with all other simulations to ensure fair testing is maintained: a steam pressure inlet, a smoke mass flow inlet, and the pressure outlet. The mesh aimed to provide a y^+ value of less than 1 on walls, illustrated in Figure 12There are two clusters of cells which exceed the scale used in the image.

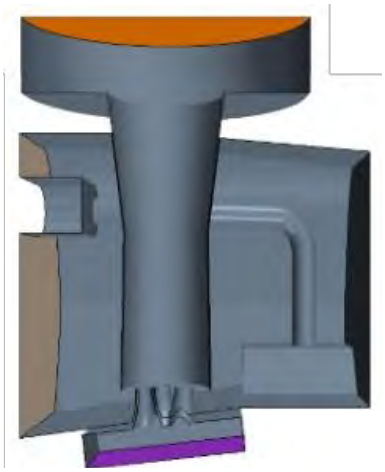

Figure 11: 7 Degree Lempor Geometry with Boundary Conditions highlighted

These were neglected as they do not enclose a critical region of the geometry. Figure 13 demonstrates the flow of air being pulled through the smokebox and under the skirt of the chimney. The extension of the chimney skirt may be too great, such that the flow is constricted as it turns into the chimney and forces the flow to undergo a significant momentum shift. The flow shows good attachment to the upper exhaust wall suggesting the diffusing angle is appropriate. A future opportunity would be to reduce the extension of the skirt and reassess the geometry's performance. The figure also demonstrates that the ejector successfully propagates the flow outwards as the nozzles are arranged, making good use of the cross-sectional area available.

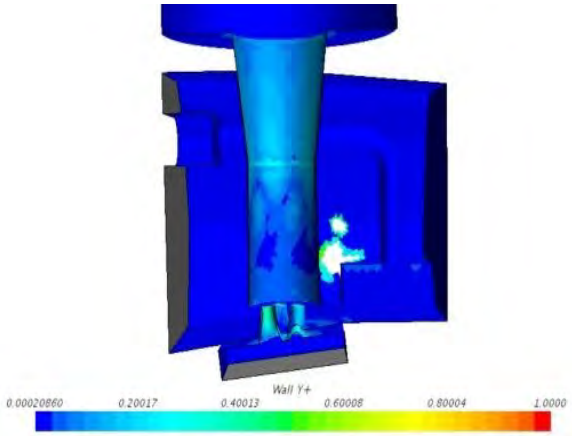

Figure 12: Contours of wall y+

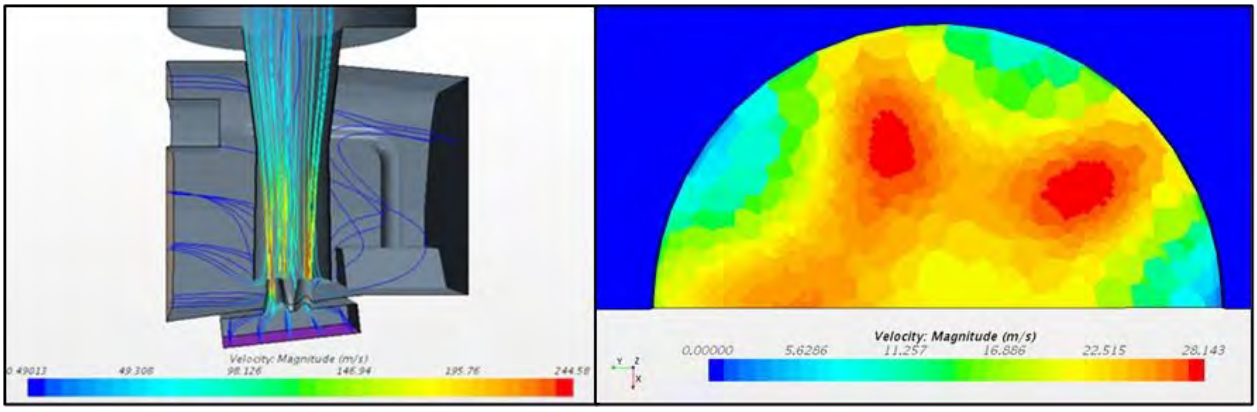

Figure 13: Geometry representation with streamlines, Exhaust Outlet Scalar Scene

5.3 The 7 Degree Giesl Exhaust

The 7-degree Giesl arrangement differs to the original design. The nozzles are no longer in circular pattern but linear. This change in nozzle arrangement impacts the external aesthetics of the locomotive as the exhaust is also affected by the new geometry. Furthermore, the Giesl design presents 7 nozzles, in comparison to the 5 in the original design.

The model setup differs slightly to the

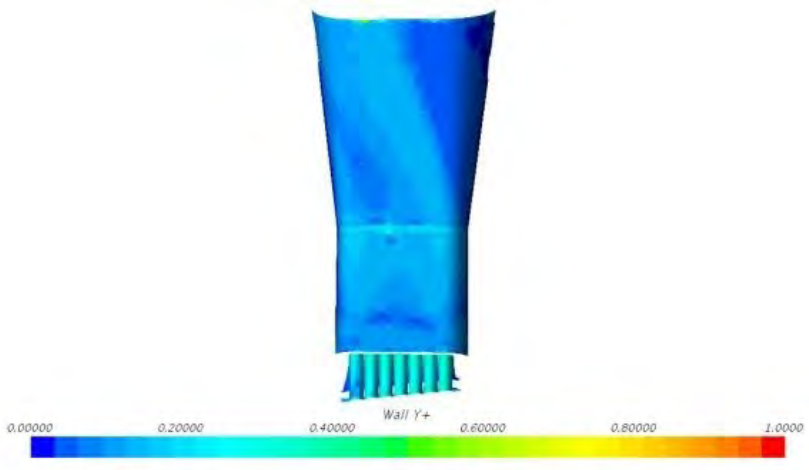

Figure 14: Wall Y+ Values for the Nozzle and Exhaust of the Giesl Ejector from the 28 000 lb/hr (Steam) Case

original design benchmark simulation. Although all physics models are used, slight adjustments to the mesh and to the boundary conditions are required to match the inlet flow rates given in the project brief. The amount of prism layers in the exhaust mesh refinement was increased from 21 to 25. This allowed all Y+ wall values to be below 1, see Figure 14, ensuring the simulated cells near the boundary layer is correct and reliable. The mesh refinement through the nozzle and the exhaust allow a higher definition of results. The change in geometry also affects the inlet stagnation pressure boundary conditions. These were recalculated for every flow rate. All residuals in the simulations were at least below 0.01, and stable, whereas some were as low as 0.0001. Clear differences are distinguishable between the Giesl and the benchmark simulations because of the change in geometry. The flow naturally behaves differently. Figure 15 provides the velocity scalar scene of the 20,000 lb/hr steam inlet and 39,600 lb/hr smoke inlet conditions of the original design compared to the Giesl ejector. It is clearly distinguishable that the flow from the Giesl ejector diverts to one side of the exhaust. There can be two potential explanations for this. Firstly, the simulation setup may be slightly flawed (use of transient

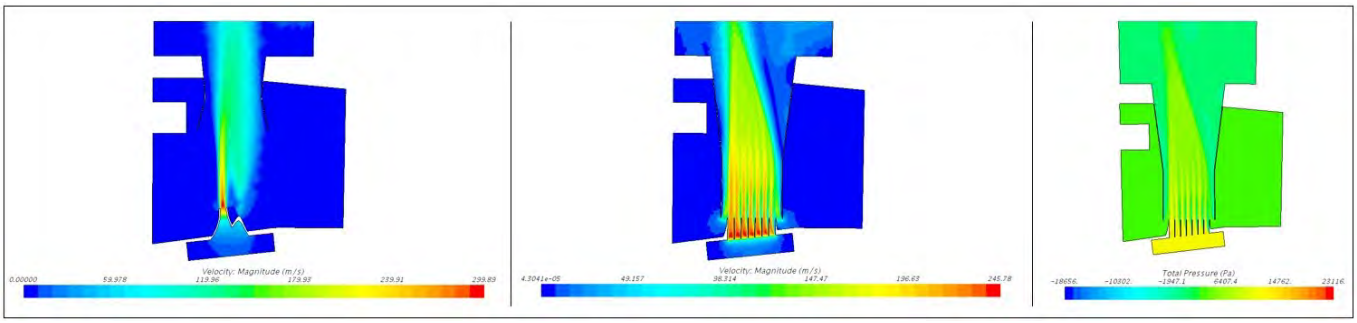

Figure 15: Velocity Contours in the Original Design (Left) & Giesl Ejector (Middle) and Pressure Scalar of the Giesl Ejector (Right).

may be more appropriate), as this problem might require the flow to be solved using different physics models, this is due to the flow separation on the righthand side of the exhaust when divergence begins. Secondly, the longer nozzle on the left provides larger speeds, this may entrain the flow from the right creating this bias. The flow streamlines can be seen in Figure 16.

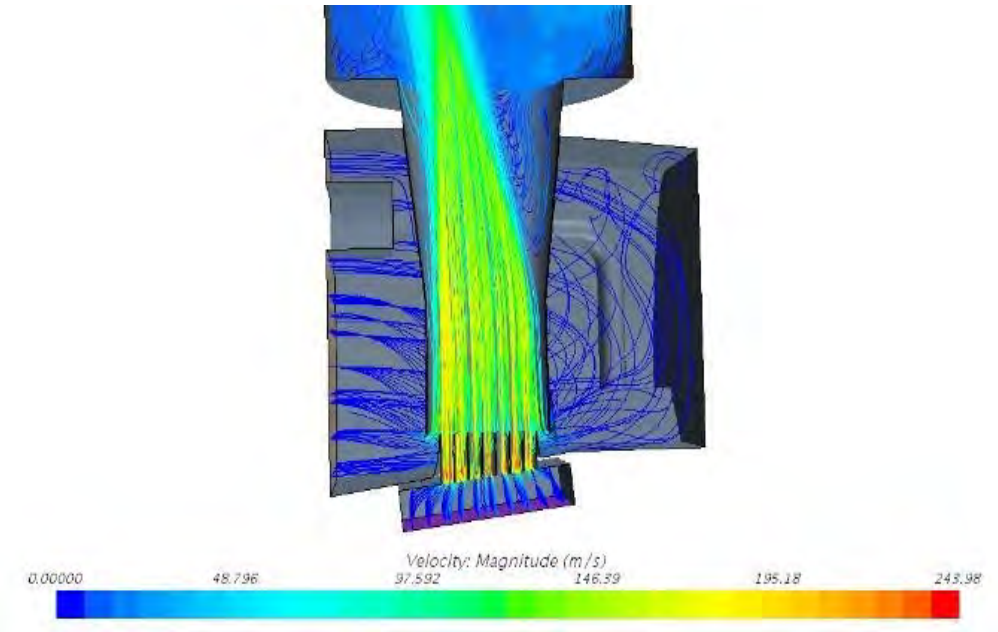

Figure 16: Streamlines within the Smokebox for the 20,000 lb/hr Steam and 39,600 lb/hr Air Case.

The mass flow rates are in correspondence with those of the original design. The pressure difference between the boiler outlet and the exhaust outlet is far greater than the benchmarked locomotive, indicating a more effective steam box, see Figure 17.

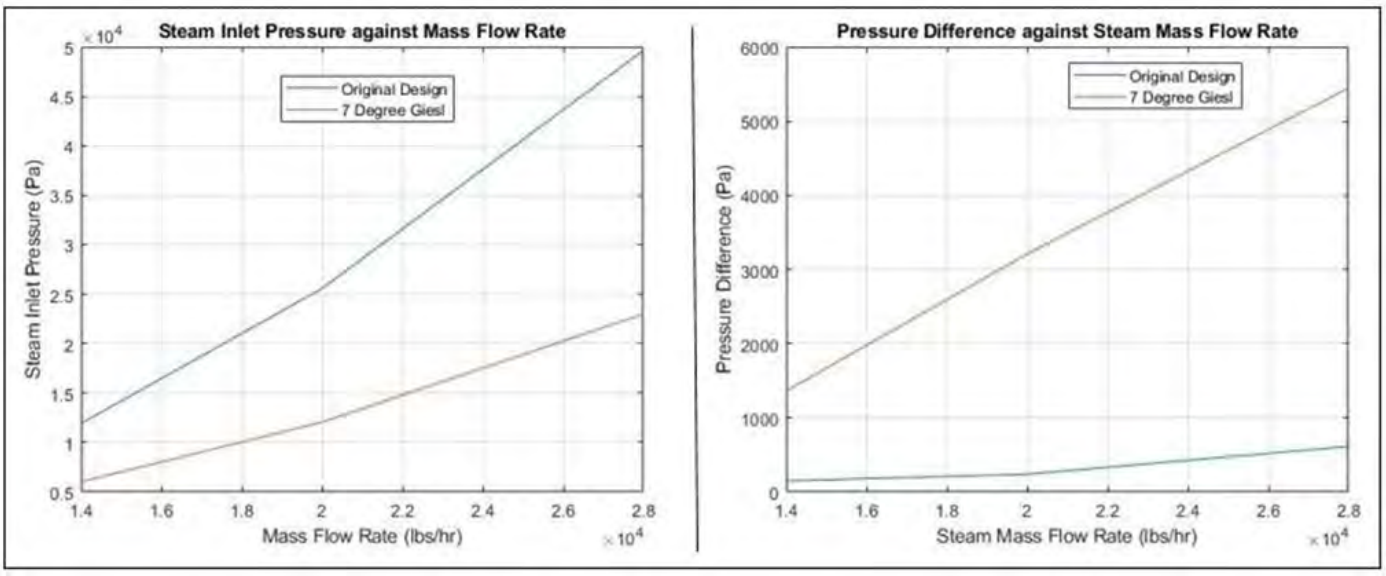

Figure 17: Inlet Pressure (Left) and Pressure Drop between Boiler Outlet and Exhaust Outlet (Right) between the Original Design and the 7 Degree Giesl

5.4 5° Degree Lempor Exhaust

This section discusses the CFD simulation results of the 5° Lempor exhaust. The main objective of this simulation is to determine its superior characteristics if any over the original design. The 5° Lempor has the same geometry as the original design, except that it has a significantly longer chimney skirt which extends almost down to the nozzles as seen in Figure 18 In comparison to the original design, the Lempor exhaust is a converging-diverging type diffuser with a relatively wide mixing chamber. The same physics models, locations of boundaries, boundary conditions, and meshing parameters as the benchmark simulation were used in order to setup a simulation that resembles the original simulation closely which makes validation and comparison of results more accurate.

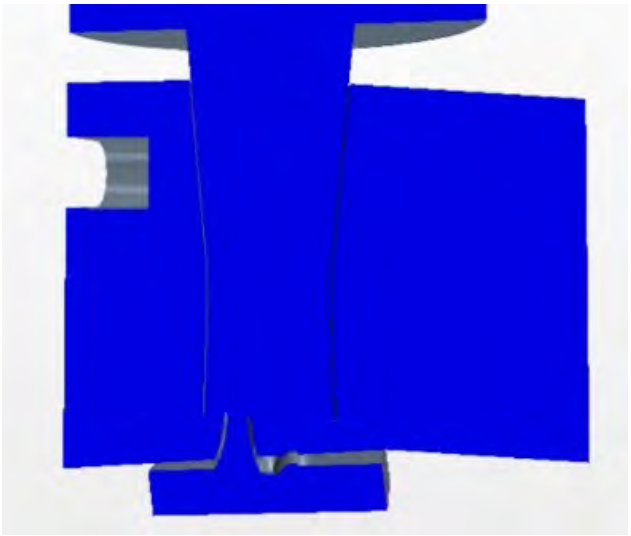

Figure 18: 5 Degree Lempor Geometry

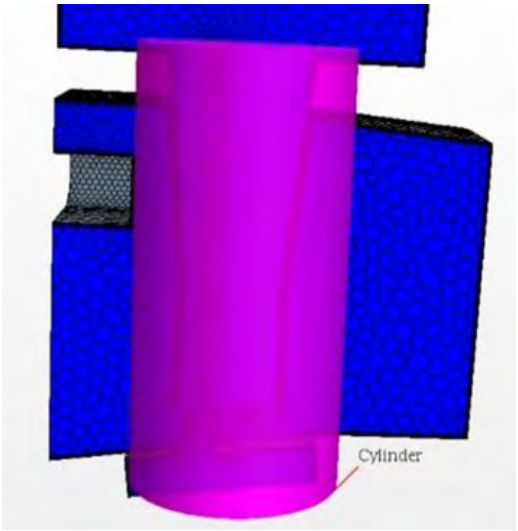

Figure 19: Mesh refinement

The same meshing models as the benchmark simulation were used, so that the differences in results if any can be attributed to geometrical changes. However, just one volumetric control cylinder was used as opposed to two in the benchmark simulation. The same mesh refinement volumetric controls were used for the section extruding from the nozzles. The same prism layer mesher settings and properties were used as in the group simulation which gave a similar mesh quality at the nozzles and near the blastpipe. As expected, the differences in the velocity flow profiles of the original design and the 5° Lempor design are easy to observe. Figure 20 illustrates the flow pattern observed on the symmetry plane. It is important to note that the decreasing trend in velocity profile differences were consistent for each set of flow rates. The peak velocity decreased for all flow rates – from 213 to 117 m/s for 14,000 lb/hr steam, from 302 to 174 m/s for 20,000 lb/hr steam, and from 408 to 246 m/s for 28,000 lb/hr steam, due to the increased flow area at the exit from the steam nozzles compared to the original design. Validation of test results was done with the help of mass averaged monitors at the exhaust and smoke inlet to help find smokebox pressure, exhaust pressure, and adjusted smokebox pressure values.

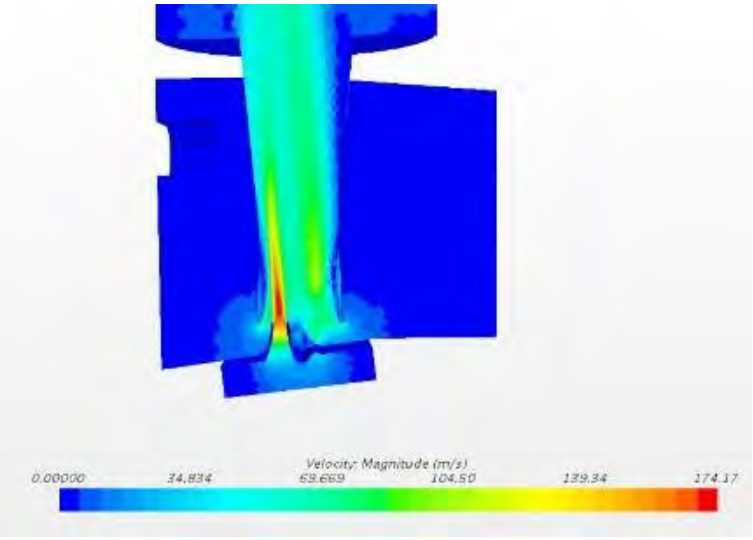

Figure 20: Contours of velocity magnitude, 5° Lempor, 20,000 lb/hr steam

6. Project Conclusion

A low steam inlet pressure is desirable as it is indicative of a low steam pressure drop through the nozzle and smoke box, meaning the steam in the cylinders needs to do less work to expel the exhaust steam. Figure 21 illustrates this metric. The Lempor designs, which have an extended chimney skirt, are grouped together at the low end of the inlet pressure scale. The shallow increase in gradient, an indication of how much the pressure needs to increase by to return a proportional mass flow rate increase, is also a positive indicator, as it shows that the geometry suffers less loss with increased mass flow rate targets. The Giesl requires an increased pressure to meet the targets, and the gradient increase is more significant than the Lempor designs, indicating a less efficient design, based on this metric.

Finally, two versions of the original design are found at the high end of the pressure scale with significant increases in gradient. The design oriented towards the centre of area delivers a marginal improvement.

Based on this data set, it may be concluded that the Lempor designs are the most desirable. But why? This may be the case of one change being explained away as the effect of another; the Lempor designs (& the Giesl) were all run with an enlarged steam nozzle exit area, to reduce the back pressure the cylinders see. Thus, it is not surprising the pressure needed in the CFD model to deliver the same mass flow is lower compared to the original design. The Giesl design is slightly worse than the Lempor, likely due to the flow maldistribution that was observed.

Figure 22 shows the pressure difference, from the boiler exit (smoke inlet plane) to a plane immediately above the exhaust outlet plane. The results are much less clear, and, by extension, less conclusive than

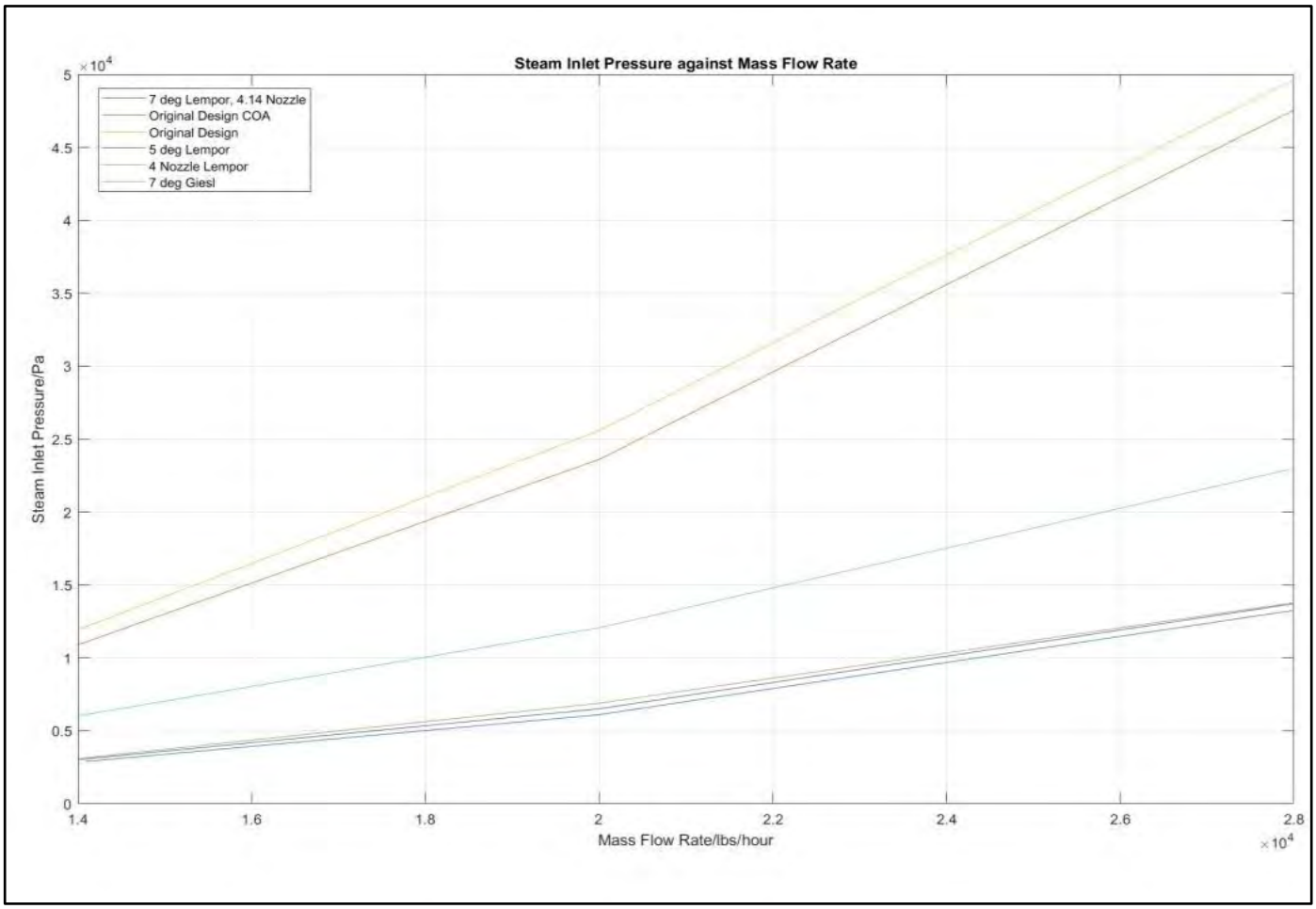

Figure 21: A Graph of Steam Inlet Pressure against Mass Flow Rate for all geometries

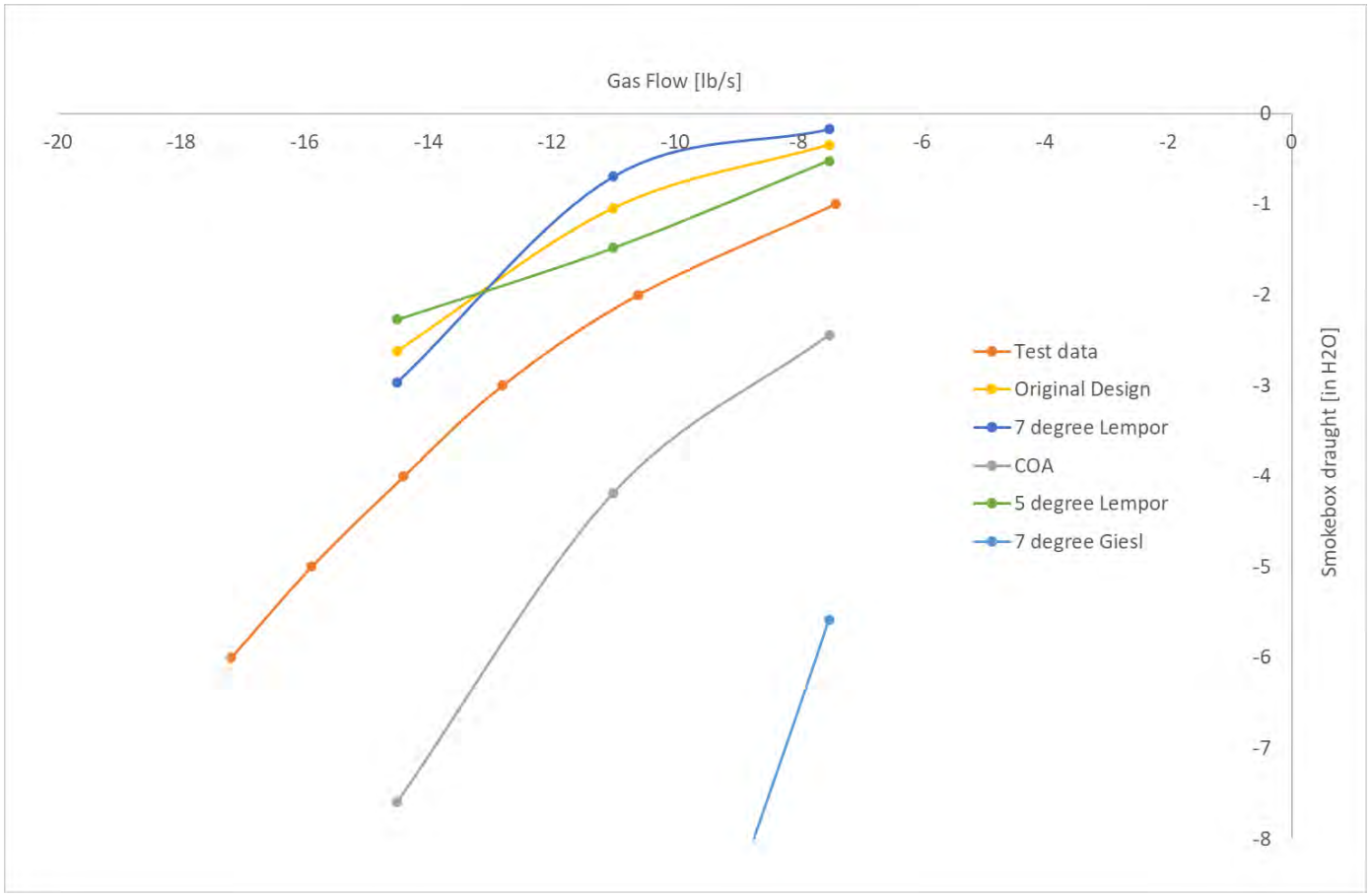

Figure 22: A Graph of Pressure Difference against Steam Mass Flow Rate for all geometries

the steam inlet pressure graph. An increase in pressure difference is desirable in this case, as it indicates the design's inclination to draw more air through the boiler, allowing for more efficient combustion (although air flow rates have been set as constants in these simulations).

The 7° Lempor design with a 4.14° nozzle, whilst exhibiting the lowest pressure difference at the lower flow rate cases, demonstrates a significant ramp up towards the highest flow rate case, suggesting that it may be best tuned to high power operation. The Giesl design clearly demonstrates a significant improvement based on the pressure difference it produces, however the result is so significant that confidence is reduced, and further work is necessary to better validate this outcome. The centre of area geometry appears to demonstrate a significant improvement on its standard counterpart, suggesting that a combination of the COA nozzle cluster and a tuned Lempor exhaust could be a particularly desirable design.

Lessons learnt and further work.

Conducting these projects remotely, due to the restrictions imposed by Covid, was a learning process. At the same time, I was also developing my understanding of the Rugby test data, the Bulleid-Lemaître exhaust design (& Lempor and Giesl designs) and adapting my previous knowledge to suit this problem. This led to not being able to arrive at a fully validated CFD methodology for multi-nozzle exhausts, reducing confidence in the results found. The study has shown that increasing the flow area of the steam nozzles, bringing them up to a value similar to that used on other Class 8 locomotives (such as the LNER A4), reduces the back pressure the cylinders will see without any obvious detriment to the draughting performance. Adjusting the angle of the nozzles has had a vast impact on the performance, possibly more than is believable at this point.

We are looking to run another project in academic year 2021/2, that will by the nature of how the projects need to be run, repeat a significant chunk of the project. My expectation of how we'll run the project (and how I would recommend others conduct similar studies) is as follows:

Firstly, we'll conduct a 2D simulation of the single-jet exhaust that was fitted to 35022 during the performance & efficiency tests. The primary flow will be as designed, the secondary will be a radial inlet, which is a simplification of conditions in the smokebox, but not a vast simplification. This can be used to develop the students' confidence & start to develop a methodology of the appropriate models to be used. Following on from this, a 3D model of either the Bulleid-Lemaître exhaust and/or the rebuilt exhaust will be produced, using the symmetry & periodicity within the design to simulate either a 36- or 72-degree sector, again with an idealised radial secondary inlet. By simulating all 3 of these designs, it is expected that a methodology that is consistent against the test data can be arrived at, which was lacking in the 20/21 attempt; the test data shows little difference between the performance of the Bulleid-Lemaître & single jet designs, with the rebuilt design producing 20% less secondary flow than the Bulleid-Lemaitre. From here, we can then look at the potential of new designs and draw on some of the lessons learnt in the 20/21 study, such as the need to provide a greater radial inlet area than some of the designs incorporated. It is likely we'll revisit the Bulleid-Lemaître with COA nozzles, as this small change produced such a significant effect on performance, it would be useful to confirm. We may also look at a Lempor type exhaust again, with a larger clearance between the base of the exhaust and the base of the smokebox. Suggestion has been made of studying a hyperbolic exhaust, as this has the theoretical

advantage of a constant rate of change of area along the axis, which would help with pressure recovery in the diffuser. Beyond this, I'm open to suggestions, though would need them very soon in order to have time to create the necessary CAD files!

Further progress continues with the re-engineering of 35011 General Steam Navigation*. On the physical side of the project, we are continuing to remove the tubes from the boiler ahead of a planned inspection later this year. The unique Merchant Navy fabricated trailing truck is ready for transport to North Norfolk Railway Engineering in Weybourne for restoration. We continue to remove the brackets from the frames that once held the Walschaerts valve gear. On the design side, we have received the results from a FEA study conducted at the University of Birmingham on the design of the crank axle, confirming the suitability of our steel choice for the axle whilst also exploring in some depth the failure that occurred on the original design. My hope is we'll be in a position in the coming months to order the forging and manufacture of the axle, a major step in returning 35011 to be a working 3-cylinder steam locomotive again.*

7. References

1. "Performance and Efficiency Tests of Southern Region "Merchant Navy" Class 3 Cyl. 4-6-2 Mixed Traffic Locomotive," British Transport Commission: British Railways, 1954.

WALL EFFECTS?
SMALL IS BEAUTIFUL
Hendrik Kaptein

This year's - again most interesting - ASTT conference included a next day visit to the wonderful Stapleford Miniature Railway. Racing along its beautiful tracks with packed passenger trains through most attractive country scenery were scaled-down versions of famous engines like a Nickel Plate 2-8-4, a New York Central Niagara and an Atlantic with no full-size forebear but then featuring fully enclosed cardan-driven valve gear, one more showpiece of Richard Coleby's superb engineering skills.

The downsized versions are original to the smallest detail, at least so in outward appearance. Mechanical lubricators and like appendages are built like finest clockwork and even fulfil their original functions, at least so in part. So well-nigh everything is just scaled down, from standard gauge to the 10¼'' Stapleford track. Nothing seems more natural of course, that is, if everything is to stay within true proportions.

Happily enough nothing much can be seen of these miniature boilers' inner construction. Just scaling down the originals would lead to impractically small firetubes, with attendant gas flow resistance if not even choking. Thus the miniature versions are rightly fitted with relatively wider firetubes, at the expense of heating surface.

But then this relative reduction of heating surface is offset by a or maybe the factor determining scaling effects: the (probably slightly counterintuitive but still inexorable) changing relationships of surface and volume, given a specific form. Probably the simplest examples of this are cubes of different sizes: with an 1'' cube the relationship of rib length, surface and volume obviously is

$1 : (6x1^2) : 1^3$

or 1 : 6 : 1. So here there is lots of surface (6'') for a small volume (1 cubic inch).

With a 2'' cube the relationships become

$2 : (6x2^2) : 2^3$

or 2 : 24 : 8. So here there is already rather more volume in relationship to surface: doubly so in fact. And so on: holding good for circular etc. forms as found in boilers, cylinders etc. as well of course.

Even without specific calculation these changing relationships imply that small boilers with (shorter and) relatively larger diameter fire tubes need not be worse in terms of heat transfer compared to larger boilers. Heating surfaces become relatively larger with smaller boilers, other things equal of course. So boiler design may not just be scaled, down or up.

This is not just a boiler issue of course. Cylinders scaled down from full-sized versions profit from better relationships between inlet and outlet areas relative to cylinder volumes, thus enabling freer "breathing" and thus better efficiency or simply better steaming. (Though some existing original designs may still be improved upon in small-scale recreation of course.)

Non-superheated condensation on the other hand will be relatively worse in smaller cylinders, as a smaller amount of steam has to cope with a relatively larger "wall" area (including the cylinder wall, one

piston side and the cylinder cover). This effect is visible in (sufficiently accurate) indicator diagrams, showing the disappearance (condensation) and reappearance (re-evaporation) of steam during the cylinder stroke. (Bill Hall noted this phenomenon but offered no explanation for it, in his paper "Measuring Steam Engine Performance" as published elsewhere on our ASTT-website.)

With superheating things become different, superheated steam being a very bad heat conductor. In fact a relatively thin outer layer only interacts with the cylinder walls. This implies that in bigger cylinders a relatively smaller part of the superheated steam acts against condensation, as an ever greater part of the total steam mass is too far away from the cylinder walls and thus cannot cooperate against this condensation. Relevant layer thickness is size-independent, hence small engines' superiority here (notwithstanding their less favorable surface / volume ratio). Simplified but still: the bigger the cylinder, the smaller the percentage of superheated steam in it acting against condensation. And the other way round of course: indeed Richard Coleby stated that superheated 10¼' gauge engines "run like the wind" (or something like it).

Still it is oftentimes but wrongly assumed that "sufficient" superheating say up to 400^{o} C does away with any wall effects (i.e. condensation and re-evaporation). Thus Bill Hall stated that "Superheat solved the practical problem by preventing condensation" (see his paper mentioned above). General steam locomotive practice was based on this mistaken assumption more or less until the very end.

This is not just an issue of a relatively small part of the total steam mass acting against condensation. Whatever the superheated steam temperature, there will always be condensation as long as the wall temperature ('wall' here indeed being generic for cylinder covers, cylinder wall and piston side) is below the steam saturation temperature at the steam pressure at the walls (± cylinder steam pressure). But the superheated steam heats up the walls it may be countered. This is only part of the story, as (again) the relatively bad heat conductivity of superheated steam precludes cooperation of the main body of it, apart from relatively thin outer layers.

So and at a given superheat temperature condensation will be worse at smaller cut-offs as well, as then there is still less steam available for properly heating up the cylinder walls. Though Porta was not the first to explain these phenomena it may still be of interest to summarize one of his empirical findings, in line with his theoretical considerations: with properly warmed-up cylinders "after a lengthy and strenuous pull" and with steam at 400^{o} C wall temperature is 210^{o} C only at cut-offs greater than 20%. (Not mentioned here by Porta is this 210^{o} C being the saturation temperature of steam at 20 at, see *Porta Papers* Vol. 2, pp. 81 ff., Chris Newman ed., ASTT. Still Porta recommends smallest possible cylinder diameters, implying long strokes, fully in line with consequences of surface / volume ratios for superheating effects as outlined above.).

Indeed wall temperatures are slightly below the mean of inlet and outlet temperatures at best (given optimal cylinder insulation). The other extreme is prolonged stand-still, leading to further decrease of wall temperatures and thus to more condensation. One more importance of (scale independent) time here is the steam-wall contact period: the shorter the better against condensation. Thus Porta recommended "the smallest driving wheels possible" in order to reduce this contact time. Generally slower running will produce more adverse wall effects, given this relationship of "contact time" and condensation.

All this may be countered by sufficiently high superheating temperatures, at least so in theory. But such temperatures are limited by combustion gas temperatures in principle and predominantly by lubrication issues in practice, still apart from ever worse heat conductivity of ever hotter steam.

Steam jackets combined with moderate superheat may be a more practical solution, both in terms of thermodynamics and in terms of maintenance (lower superheat lessening lubrication problems etc.). Such steam jackets have in fact been suggested for *Revolution*. But then the disadvantages of this added complexity probably outweigh any thermodynamical gains, given *Revolution*'s relatively small scale.

So and to conclude: any design and any performance prediction (like Bill Hall's *Perform* and *Perwal*) ought to include scaling factors, at least so concerning superheating at feasible temperatures up to 400°+ C. Bill Hall himself took it for granted that superheating prevents wall effects (as quoted above and possibly based on his experience with a small scale engine indeed). To the extent that *Perform* and *Perwal* are based on this assumption it may make sense to further improve them, in order to take scaling factors into account, possibly not just concerning superheating.—A "small" issue maybe, but hopefully sufficiently interesting in our full-scale steam world.

Historical note: As far as the present author is aware of Porta did not mention Chapelon's more extensive treatment of superheating and wall effects, though both are in full agreement on these subjects: see *La Locomotive à Vapeur* (1938 edition), pp. 619-628. Chapelon in his turn readily conceded that his results were not new, given the complete establishment of superheating and wall effect theory by Hirn and others in the late 19th century, though nothing was done with it in steam locomotive practice. (Specific application of such thermodynamics is another matter of course, nowadays greatly furthered by computer modelling). In fact the principles of superheating were already published by Denis Papin, in 1707. "He who does not know the history of technology is doomed to repeat it"…

MAINLINE & MARITIME

THE UK'S ONLY WORLDWIDE RAILWAY MAGAZINE PRODUCED BY ENTHUSIASTS FOR ENTHUSIASTS

SIX ISSUES PER YEAR

RRP £5.95 UK SUBSCRIPTION £32
www.locomotivesinternational.co.uk